DESIGN OF A HIGH-SPEED INDUCTION GENERATOR

by

WILLIAM H. GABLE

S.B., Massachusetts Institute of Technology
(1951)

SUBMITTED IN PARTIAL FULFILLMENT OF THE

REQUIREMENTS FOR THE DEGREE OF

MASTER OF SCIENCE

at the

MASSACHUSETTS INSTITUTE OF TECHNOLOGY
(1953)

Signature of Author _____
Department of Electrical Engineering, January 19, 1953

Certified by _____
Thesis Supervisor

_____
Chairman, Department Committee on Graduate Students

DESIGN OF A HIGH-SPEED INDUCTION GENERATOR

by

WILLIAM H. GABLE

Submitted to the Department of Electrical Engineering on January 19, 1953, in partial fulfillment of the requirements for the degree of Master of Science.

ABSTRACT

The thesis discusses the design of a 60,000 rpm induction alternator. Specifications require the machine to operate as a motor and also to deliver one to two kilowatts of electrical power as a capacitor-excited induction generator. A general discussion is included which outlines the initial choice of dimensions, flux density, and current density for induction machines with the emphasis on short duty cycle, high-speed machines. The discussion presents an energy rather than a voltage approach and per-unit reactance quantities rather than ohmic reactances in an attempt to normalize and systematize the initial designing process.

Calculated curves are presented for determining the effective resistance of round copper conductors in a-c armature and transformer windings. Curves of zig-zag permeance factor and stator and rotor gap factors for various configurations of air-gap geometry are included.

A detailed description of the 60,000 rpm induction machine is presented. Salient features are the overall dimensions (4 inches in diameter and 4 inches long), the large air gap (1/32 inch), and the transformer incorporated in the stator to allow excitation and distribution voltages that are different. Included is a generator equivalent circuit in which the circuit constants are calculated from design quantities and checked by conventional blocked-rotor and no-load tests.

Also presented are the results of motor-load tests over a speed range of 12,000 to 24,000 rpm and induction generator tests over a speed range of 18,000 to 42,000 rpm. The turbine and isolated-induction-generator combination exhibited good inherent operating stability with decreases in load resistance or excitation capacitance. Test results indicate that the induction alternator will meet its design requirements at 60,000 rpm, and that machines of this type have many practical applications where high power output per unit volume is required.

Thesis Supervisor: David C. White
Title: Assistant Professor of Electrical Engineering

ACKNOWLEDGMENT

The author wishes to express his appreciation for the assistance and cooperation he received during the design, construction, and test of the induction machine.

Professor David C. White encouraged and counseled the author in the initial investigation of basic machine types and throughout all the stages of the thesis investigation.

The author is indebted to the personnel of the Dynamic Analysis and Control Laboratory for making possible the construction of the machine and assisting in its design and test. In particular the assistance of Mr. Robert W. Mann in matters of mechanical design and of Mr. Sherman K. Grinnel in setting up and running tests in the Gas Turbine Laboratory is greatly appreciated.

Mr. Roger B. Bross of the Instrumentation Laboratory helped considerably by presenting the author with a copy of his "Notes on the Design of Polyphase Induction Motors".

The cooperation of Mr. James H. Grimes of the Aeronautical Engineering Department in supplying power for the motor load tests is greatly appreciated.

TABLE OF CONTENTS

LIST OF ILLUSTRATIONS

I

INTRODUCTION

The purpose of the thesis investigation is the design of a capacitor-excited high-speed induction generator and the determination of general design techniques and limitations of such machines. The problem grew out of the need for a high-speed alternator to meet the following requirements:

(1) Deliver one to two kilowatts of electrical power for about one minute

(2) Operate at an approximate speed of 60,000 rpm with an output frequency of 1000 to 3000 cps

(3) Have the minimum volume possible

(4) Be capable of operating as a motor to bring the prime mover to operating speed and drive it in a standby condition for approximately fifteen minutes

Four basic types of alternators were considered; the conventional wound-field type, the permanent-magnet type, the inductor or variable reluctance alternator and the induction generator. The difficulties of balancing the wound rotor and keeping rotor windings in place at the high rotational speeds make a wound rotor impractical for this application. The problems of wound rotor construction at high speeds have also been found in industry where some of the manufacturers of aircraft generators have experienced development difficulties at 24,000 rpm. The permanent-magnet type will not operate as a motor without the addition of a starting

winding on the rotor and has the further disadvantages that voltage control is difficult, demagnetization of the permanent-magnet material under transient conditions is possible, and the mechanical properties of common permanent-magnet materials are barely sufficient to withstand the high-rotational stresses. The inductor alternator is essentially a low-speed, high-frequency device. The output frequency is determined by the number of rotor slots with one slot constituting a pair of poles in the conventional sense. Hence a rotor designed for 1000 cps at 60,000 rpm would have only one slot and lowest practical output frequency at this speed is 2000 cps. The inductor machine would not start as a motor in its usual form and the excitation flux is at best only half as effective as in the conventional alt. .nator.

A squirrel-cage induction motor when driven mechanically will deliver electrical power providing excitation is supplied from static capacitors or over-excited synchronous machines. Such an induction generator has a rugged-rotor construction and the recognized ability to deliver mechanical power as a motor. Because of these advantages, an induction generator was designed and built.

The electrical designer thinks and works in terms of the dimensions of a stack of iron laminations, winding current densities, flux densities, permeances of various air and iron flux paths, and copper and iron losses. He must be also familiar to a lesser degree with heat storage and dissipation, mechanical stress limitations, critical speeds of rotation, and friction and windage effects. Specifications for an a-c machine, on the

other hand, are usually stated in terms of power, voltage, frequency, and speed requirements; efficiency and power factor; allowable operating life or temperature rise; volume or weight limitations; allowable cost; inherent voltage and frequency regulation for a generator; and inherent speed regulation for a motor.

Unfortunately, it is not presently possible to synthesize the optimum machine for a given set of specifications in one operation. In its present form, the designing art is a cumbersome cut and try process in which the designer may spend hours trying to mold a poor initial choice of dimensions into an acceptable design. A definite improvement over this technique is an approach which allows the designer to rise above the tedious trial and error calculations, make an optimum or nearly optimum selection of basic machine dimensions, and then complete what detailed design work remains. This type of approach requires initial designing in terms of power or volt amperes and normalized or per-unit reactances rather than volts and amperes and ohmic values of reactances. Throughout this investigation attempts were made to improve the initial design approach and to replace tedious calculations by graphical plots wherever possible. The emphasis throughout is on high-speed, short-life induction machines.

II

THE INITIAL CHOICE OF DIMENSIONS

In an induction machine a certain product of rotor length and diameter, air-gap flux density, stator current density, total stator conductor cross-sectional area, and winding factor is required to meet specified power, power factor, efficiency, and speed requirements. For a generator in particular the following equation can be derived: (The complete derivation is given in the Appendix.)

$$k_w A B_g D L S_c = \frac{27 \times 10^8 (VA)}{n} \qquad (1)$$

where k_w = the winding factor = the product of pitch and distribution factors

A = the stator current density in amperes/in^2

B_g = the air-gap flux density in lines/in^2

D = the rotor diameter in inches

L = the rotor stack length in inches

S_c = the total stator-conductor cross-sectional area in in^2

(VA) = the rated output volt amperes of the generator

n = the synchronous speed in rpm

The winding factor depends on the desired area of the end turns and harmonic pitch and distribution factors. A choice of number of poles, stator slots, and winding pitch must be made before the pitch and distribution factors can be calculated. Generally this factor will lie between 0.75 and 0.90 and an initial value in this range can be chosen for preliminary calculations.

The stator current density depends primarily upon the allowable temperature rise in the stator windings. For relatively long life or continuously rated equipment the density is limited by the amount of heat that can be removed by radiation, conduction, and in some cases forced convection so that a specified steady-state operating temperature can be reached. In such cases the density is largely dependent upon empirical data and loss coefficients and may range from 2000 amperes/in^2 for totally enclosed machines to 10,000 amperes/in^2 for machines with forced ventilation. For short life equipment with ratings of a few minutes or less, thermal equilibrium is never reached, and a useful approximation can be obtained by neglecting heat dissipation altogether and assuming that all of the power loss goes into heat storage in the conductor and hence into raising the conductor temperature. What this amounts to is using as a first approximation the initial slope of a more or less exponential heat rise curve. With this approach the following equations can be derived: (The complete derivation is given in the Appendix.)

For copper: $$A = \sqrt{\frac{1.15 \times 10^6 \, \theta}{t}} \qquad (2)$$

For aluminum: $$A = \sqrt{\frac{0.49 \times 10^6 \, \theta}{t}} \qquad (3)$$

where A is the allowable current density in amperes/in^2 for a rise of θ degrees Centigrade in t minutes.

The choice of air-gap flux density is determined by the maximum allowable density in the stator teeth. This may be limited from either an excitation or core-loss standpoint. In low frequency machines the former is more likely to be the limit, whereas at high frequencies, core

loss will serve to set the tooth density. The core loss in the teeth depends upon the grade of stator iron (per cent silicon content), thickness of laminations, stacking factor, type of inter-lamination insulation, allowable temperature rise in the iron, and punching quality of the material at various thicknesses. For short life applications higher core losses are permissible. The same reasoning mentioned above can be applied and the following formula derived:

(The complete derivation is included in the Appendix.)

$$p = 3.75 \frac{\theta}{t} \qquad (4)$$

where p = watts/pound

θ = temperature rise in degrees C

t = time in minutes

The core loss in watts/pound as a function of flux density, lamination thickness and frequency can be found in the publications of the various producers of electrical-sheet steel. Once the tooth density has been set, the gap density can be taken as 25 to 40 per cent of the chosen value.

The factors affecting the diameter, length and conductor section are all interrelated. A useful simplification of some of the interrelations can be obtained by realizing that the product of length and stator-conductor section is equal to the total volume of copper or aluminum in the stator-lamination stack. Here then is the key to the design of an induction machine. For given volt-ampere, operating life, frequency, and speed requirements the current and flux densities can be chosen in the manner described previously and the designing process reduced to the

best evaluation of the product of rotor diameter and stator conductor volume. This product is influenced by the following factors:

(1) Mechanical stress limitations in the rotor laminations and end rings set the maximum rotor diameter for a given operating speed. The electrical machinery designer should have some knowledge of where these stress limitations are important. In Figure 1 is shown a plot of the maximum stress in steel laminations as a function of rotor diameter and speed. The plot is calculated from an equation for the maximum stress in a thin rotating disc included in Part II of Timoshenko's book "Strength Of Materials". In the calculation it was assumed that the inner and outer radii were approximately equal. For the case where the outer radius is much larger than the inner one, the stress values are high by 20 per cent. The maximum rotational stress given by the graph occurs at the inside diameter of the laminations. In some instances it might be possible to allow the maximum stress to actually exceed the yield stress of the material and accept a small amount of local yielding at the inside diameter. The yield stress increases with the silicon content so that the use of a good grade of electrical-sheet steel for rotor laminations allows a larger rotor diameter.

The end ring stress can be calculated from the simple hoop tension formula which reduces to the following equations for copper and aluminum:

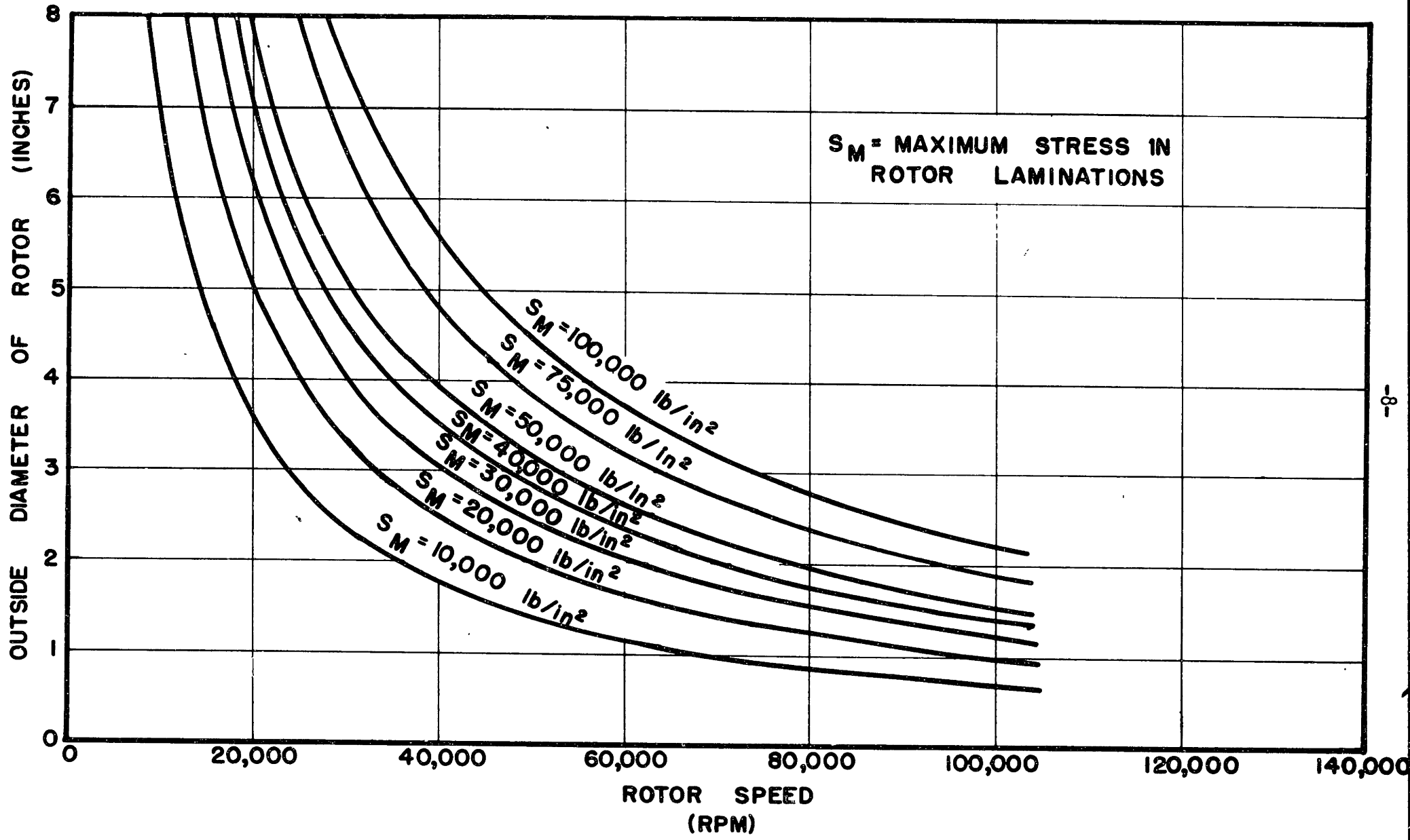

Fig 1 Maximum rotation stress in steel laminations as a function of rotor diameter and speed.

copper: $S_{er} = 2.28 \times 10^{-6} (D_{er}\, n)^2$ (5)

aluminum: $S_{er} = 0.67 \times 10^{-6} (D_{er}\, n)^2$ (6)

where S_{er} = stress in end ring in pounds/in^2

D_{er} = mean diameter of end ring in inches

n = rpm

In cases where the end ring stress is greater than the yield stress for the material, a disc type end ring can be easily supported. Care must then be taken in calculating the effect on the rotor resistance of the non-uniform current distributions set up in such a ring. A method of taking this into account is presented in Trickey's paper, "Induction Motor Resistance Ring Width".

The centrifugal stress in the rotor teeth should also be checked, although in the various designs completed, it was generally found that a reasonable flux density from an excitation standpoint resulted in a safe working stress in the rotor teeth. The maximum tooth stress can be easily approximated by calculating the rotational force exerted on one rotor tooth by the mass of iron and rotor bar supported by the tooth and then dividing the force by the minimum tooth area.

(2) A minimum volume requirement forces the designer to minimize the rotor diameter as much as possible since volume is proportional to D^2L. However, as shown previously, as diameter is

decreased the stator conductor volume must be increased to meet the specified volt-ampere and speed conditions. If the conductor cross section could be kept constant with decreases in diameter, the length would simply be inversely proportional to the diameter. Such is not the case because the conductor cross section cannot be kept constant with decreases in diameter. One of two limiting factors will force a decrease in the conductor cross section. First, for a given diameter, the maximum slot width is set by the allowable tooth density, and increases in winding area can only be bought at the expense of increased slot depth which in turn means a larger slot permeance and hence, a larger slot leakage reactance. Second, sufficient area must be left in the rotor laminations to accommodate the rotor conductor volume. It is true that higher current densities are permissible in the rotor bars because the slip-frequency core losses and lack of winding insulation allow the rotor iron to serve as a heat sink for the rotor I^2R losses. Nevertheless, in several of the designs carried out, rotor conductor section turned out to be the limiting factor. One method of solution to this problem particularly applicable to the large-air-gap-type induction machine discussed subsequently is to use a thin aluminum cylinder for the rotor conductor and to shrink this over the rotor stack. The possibility that such a rotor conductor may even serve to damp out the high-frequency harmonics due to stator-slot openings and hence, reduce the associated

high-frequency core losses at the rotor surface is certainly worthy of analytical and experimental treatment.

(3) Leakage and magnetizing reactance requirements may serve to determine both the ratio of diameter to length and the minimum diameter and length that can be tolerated for satisfactory machine performance. Unfortunately, in many design texts, leakage reactance is often relegated to a position of secondary importance and is calculated almost as an afterthought. Such a process may work well for 25 or 60 cycle machinery but cannot be safely applied to 1000 to 10,000 cycle machines, particularly induction motors where the maximum mechanical output power depends primarily on the per-unit-leakage reactance. To emphasize this effect, maximum internal power as a function of leakage reactance is plotted in normalized form in Figure 2 for various combinations of machine parameters.

Because of the importance of machine reactances, a subsequent section is devoted to a discussion of the design parameters affecting reactance. Judicious design techniques can reduce leakage-inductance permeances to a minimum for a certain length, diameter and air-gap flux combination but further gains can be realized only through increases in machine volume. The following equations derived in the Appendix show in normalized form the quantities which influence the three principle-machine-leakage reactances and the magnetizing reactance.

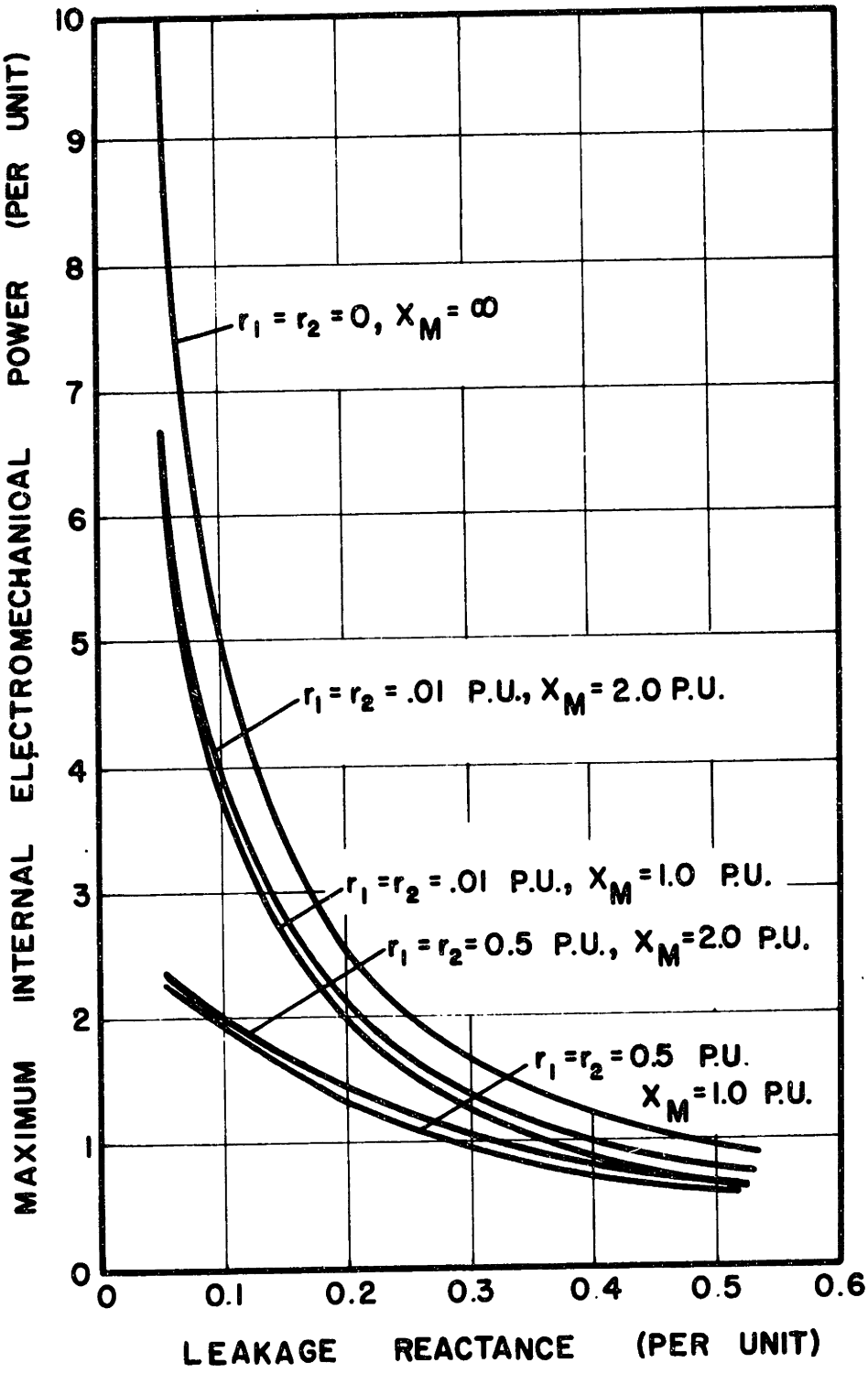

Fig 2 Maximum electromechanical power vs per unit leakage reactance for an induction motor.

$$\text{Per Unit} \quad X_s = \frac{1.02\, p^2\, (VA)\, K_s \times 10^8}{f\, B_g^2\, D^2\, L\, S_s} \tag{7}$$

$$\text{Per Unit} \quad X_{zz} = \frac{0.339\, p^2\, (VA)\, K_{zz} \times 10^8}{f\, B_g^2\, D^2\, L\, \delta\, S_s} \tag{8}$$

$$\text{Per Unit} \quad X_e = \frac{0.500\, (1 + d_s/D)\, p\, (VA)(CT) \times 10^8}{f\, B_g^2\, D\, L^2\, S_s} \tag{9}$$

$$\text{Per Unit} \quad X_M = \frac{0.325\, (VA) \times 10^8}{k_s\, k_r\, k_{sat}\, f\, B_g^2\, D\, L\, \delta} \tag{10}$$

where

X_s = slot leakage reactance

X_{zz} = zig-zag or tooth tip leakage reactance

X_e = end turn leakage reactance

X_M = magnetizing reactance

p = number of poles

K_s = slot shape factor

f = frequency in cycles/second

S_s = number of stator slots

K_{zz} = air gap geometry factor

δ = air gap length in inches

d_s = stator slot depth in inches

(CT) = coil throw in number of slots

k_s, k_r = stator and rotor gap factors (discussed in leakage reactance section)

k_{sat} = saturation factor = $1 + \frac{(AT)_{iron}}{(AT)_{gap}}$

Several things are immediately evident from the equations. For a given D L product and flux density, one way to minimize leakage reactance is to increase the diameter. An increase in the number of slots does not bring about the corresponding gain that might be expected from the equations because K_s and K_{zz} both contain factors which nullify the increase in slots, and coil throw also increases in proportion to the number of slots. Since $\frac{f}{p}$ is proportional to speed, the equations show that for a specified rotational speed the minimum leakage reactance can be obtained with a two pole design.

Thus in an induction machine a large number of factors must be considered in the initial choice of dimensions. As outlined above, this initial thinking can be completely independent of voltage considerations, number of turns, number of phases, and winding layout and still give accurate insight into actual machine performance.

III

DESIGN OF THE WINDINGS

Once the densities, principle dimensions, and conductor cross section have been selected, the next step is the design of the windings. The current per phase can be calculated from the following equation:

$$I = \frac{(VA)}{m E} \qquad (11)$$

E = volts per phase
m = number of phases
I = amperes per phase

The series turns per phase can then be found:

$$N = \frac{S_c A}{2 m I} \qquad (12)$$

N = series turns per phase

And the wire size can be determined from the conductor area:

$$s_c = \frac{I}{A a} \qquad (13)$$

s_c = area of one conductor in inches^2
a = number of parallel circuits per phase

With this information the conductors per slot or turns per coil can be easily calculated as described in Kuhlmann or Gray's design text.

At this point the designer should check the skin effect in the stator windings. In 60 cycle machines the eddy-current effect usually causes an increase of 10 to 15 per cent in the d-c resistance value. At high frequencies the effective resistance of poorly designed windings may be two or more times the d-c value. For short-life equipment this could mean a temperature rise in the conductors twice as high as that predicted from equations (2) or (3). Fortunately, most low-power (one to two kilowatt)

transformers or machines with voltage ratings in the 150 volt range and up will automatically have low-eddy-current losses for frequencies of 400 to 2000 cps because of the range of wire sizes involved. The reason for this can be clearly seen if one examines any of the theoretical discussions of eddy-current phenomena in iron-core devices such as that of H. W. Taylor in his paper, "Eddy Currents in Stator Windings", W. V. Lyon in his paper, "Heat Losses in the Conductors of Alternating-Current Machines", or H. B. Dwight in his book, "Electrical Coils and Conductors". In each case it is shown that the fractional increase in resistance is proportional to the fourth power of the conductor thickness in the direction perpendicular to the flux which crosses the conductor. In a-c armature windings this flux is the slot-leakage flux which crosses horizontally for the case of a slot pointing vertically upward. The eddy current loss is also proportional to the square of the following quantities: frequency, per unit conductor width, and number of conductors perpendicular to the direction of flux.

Approximate values of effective resistance of armature windings can be obtained from Figure 3. The eddy current loss can be calculated by multiplying $(\frac{R_{AC}}{R_{DC}} - 1)$ times $R_{DC}I^2$ or simply taking the product of $R_{DC}I^2$ and $c\beta$. With a few simple modifications, the graph in Figure 3 can also be used to find the effective resistance of transformer windings. For transformers

$$R_{AC} = (1 + \beta) R_{DC}$$

q = two times the number of layers of windings

n = the number of turns per layer

and S = the length of the stack of turns measured parallel to the mean length of iron.

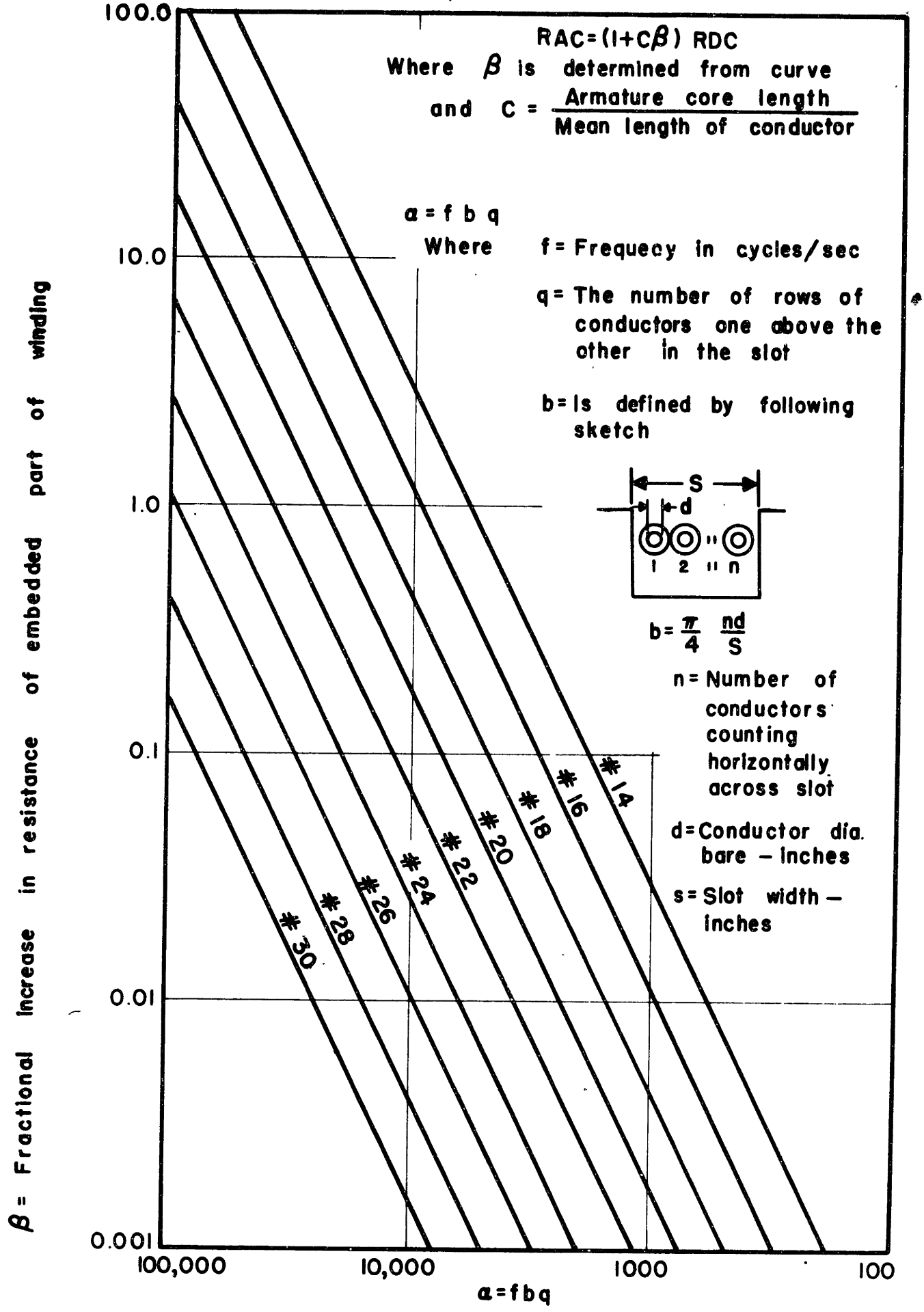

Fig 3 Effective resistance of armature windings.

The calculations for the graph are explained in the Appendix. The two assumptions made in the calculations of the graphical values were that higher-order terms than the first in the converging Bessel series, which is the solution of the differential equation for effective resistance, were negligible; and that in the case of polyphase machines all of the slots contained windings of the same phase in the upper and lower portions of the slot. The first assumption is valid if $d^2 < \frac{10}{f}$ where d is the bare-wire diameter and f is the frequency, and the maximum possible error for the second assumption is about 20 per cent and occurs if none of the slots have windings of the same phase in the top and bottom.

Since $(\frac{R_{AC}}{R_{DC}} - 1)$ is proportional to the fourth power of the conductor diameter (for round wire), the easiest method of correcting an excessive eddy-current loss condition is to replace the conductors with smaller conductors in parallel. When separate form-wound coils are made up for the armature windings and two or more conductors in parallel are used to reduce the eddy-current loss, it is safer not to have the laminations or parallel conductors shorted together at the ends of each coil. The reason for this is that the amount of leakage flux which links a conductor varies considerably with the depthwise location of the conductor in the slot. If the parallel conductors are soldered together at the beginning and end of the coil, circulating eddy currents flow along the upper conductors and return along the lower ones, thus providing an increased copper loss in all parts of the coil in addition to the eddy-current loss in the embedded part. If the conductors are carried completely through the entire winding

and then connected together, this effect will be balanced out by the random twisting of the wires and the random placement of the parallel conductors in the slots throughout the entire winding.

IV

RELATION OF MACHINE REACTANCES TO DESIGN

As mentioned previously, the performance of induction machines is to a very large extent determined by the leakage reactance. For motor operation the leakage reactance sets the maximum internal power available, and for generator operation the leakage reactance primarily determines the inherent voltage regulation. In general it is desirable to keep the mutual or magnetizing reactance as large as possible while minimizing the leakage reactance.

In high-frequency induction machines, the reduction in the air-gap flux density to reduce iron losses usually results in increases in the per-unit leakage reactance. The reasons for this can be seen from equations (1), (7), and (8). In equation (1) a given volt-ampere and speed requirement makes $B_g DLS_c$ equal a constant if A and k_w have been selected. A decrease in B_g means that DLS_c must increase. In the denominator of equations (7) and (8) the factor $B_g^2 D^2 L$ appears. If D alone were increased to compensate for the decrease in flux density, the leakage reactances would be unchanged. However, an increase in D makes more stator conductor area available and, therefore, L could be decreased resulting in higher per-unit leakage reactances. On the other hand, if L alone were increased to compensate for the decrease in B_g, the factor $B_g^2 D^2 L$ would be reduced and the leakage reactance increased. Of course if D or L were increased by an amount greater than that needed to

compensate for the reduction of B_g in equation (1) or if S_c were kept constant with increases in D, the leakage reactance could be kept constant or reduced. However, this means that the machine volume is not optimized since leakage reactance rather than volt-ampere rating is setting the minimum volume.

To reduce leakage reactance, the designer should be familiar with the permeances of the slot and zig-zag leakage paths so that these can be reduced as much as possible. Graphical plots of slot permeance for various slot configurations can be found in Kuhlmann's design text. In general, reductions in slot permeance can be accomplished by following the more or less common sense rule of keeping the width to depth ratio for various sections of the slot a maximum. It will prove necessary in most designs to use partially closed slots to reduce the undesirable effects of large slot openings such as high-frequency rotor tooth-tip core losses, synchronous lock in torques, and cusps in the torque-speed curve. Totally-closed rotor slots are not feasible in high-frequency machines because the bridge at the top of the slot is more difficult to saturate at the lower flux densities used in such machines, and hence rotor slot leakage would be excessive. Higher rotational speeds tend to rule out closed rotor slots from a mechanical standpoint.

Reducing the number of slots reduces the slot leakage slightly. A glance at equation (7) shows that if the number of slots is halved, the slot permeance factor K_s must be decreased by a factor greater than two to bring about a reduction in slot leakage. This can be accomplished because less overall area is taken up by slot insulation where fewer slots

are used and hence the slot depth can be reduced. Also the permeance in the neck of the slot can generally be decreased by more than one-half. The disadvantage of this technique, however, is that it becomes more difficult to produce a sinusoidal flux distribution with fewer slots. This can be partially overcome through careful distribution of the windings.

The geometry of the slot openings and air-gap length affects the permeance of the zig-zag and slot-leakage-flux paths and the magnetizing or mutual flux path. Figure 4 is a plot of $\frac{K_{zz}}{\delta}$ for various configurations of air-gap geometry. The calculations for the graph are explained in the Appendix. For a certain combination of flux density, diameter, and length, Figure 4 shows that the zig-zag permeance can be minimized through the use of large air gaps and slot openings. The leakage flux across the neck of the slot is also minimized with large slot openings. The magnetizing reactance is inversely proportional to the product $k_s k_r \delta$ which depends upon air-gap geometry. k_s and k_r are factors greater than unity which correct for the effect of slot openings. The following equations for k_s and k_r were derived from Carter's work by Professor Dwight:

$$k_s = \frac{1}{1 - \frac{a_s^2}{b_s(5\delta + a_s)}} \qquad (14)$$

$$k_r = \frac{1}{1 - \frac{a_r^2}{b_r(5\delta + a_r)}} \qquad (15)$$

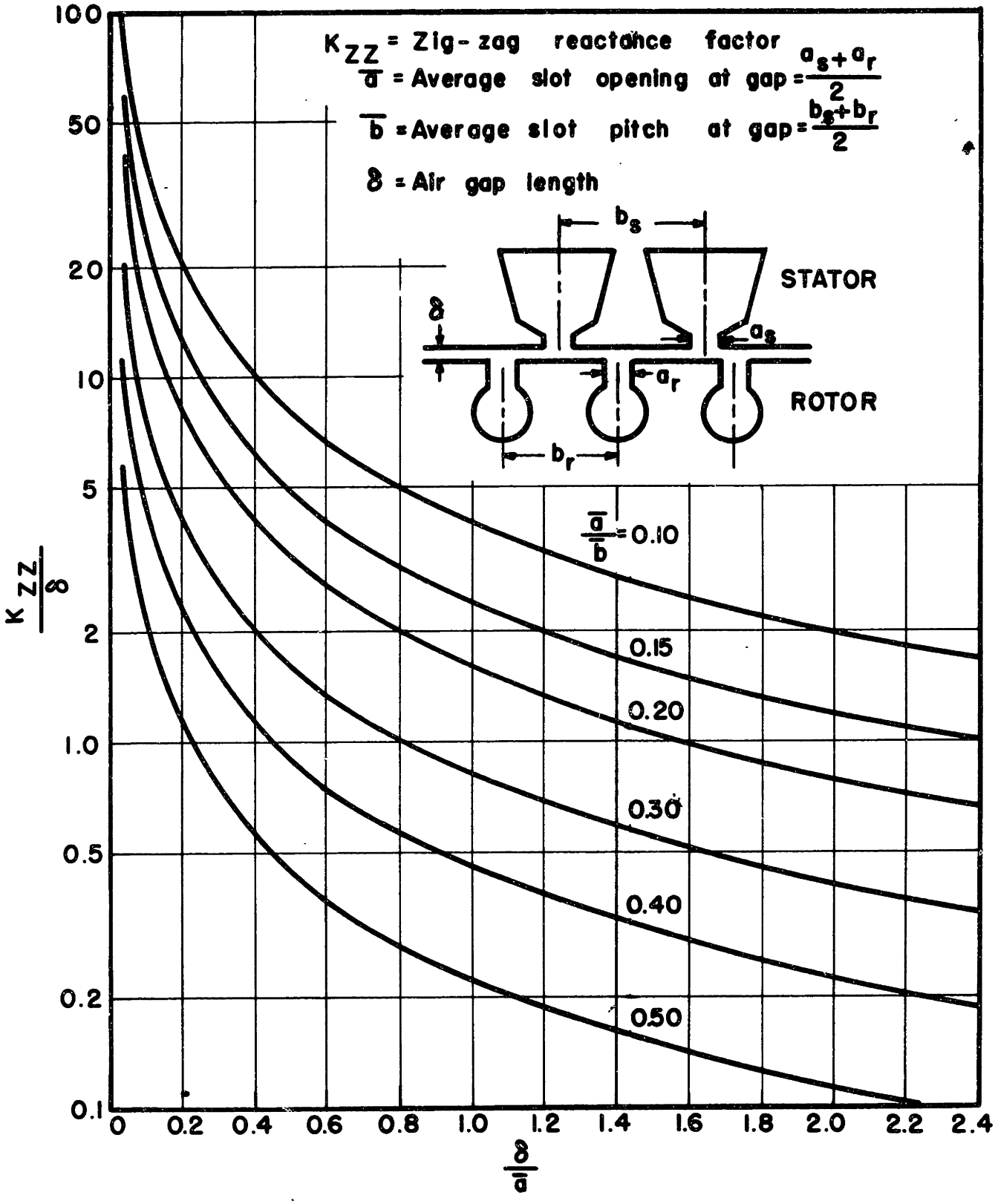

Fig. 4 Ratio of zig-zig reactance factor to air gap length for various configuration of air gap geometry.

a_s, a_r, b_s and b_r are the same as described in Figure 4. These equations are plotted in normalized form in Figure 5 to facilitate a rapid evaluation of k_s and k_r for various values of slot opening and gap length.

It is desirable to keep the magnetizing reactance as large as possible while reducing the leakage reactance. Because both the zig-zag and magnetizing reactances are inversely proportional to gap length, the design must be largely a compromise between these two quantities. The usual trend in induction motor design is to make the air gap as small as mechanical construction will allow. At 60 cps the high flux density prevents zig-zag leakage from becoming a problem. Such small gaps in high frequency machines lead to excessive zig-zag leakage unless the reduction in gap density is entirely compensated for by a volume increase. Even if this is done, other problems of small gaps such as high frequency tooth-tip losses, synchronous locking, and cusps in the torque-speed curve due to slot openings are still present.

A different design approach for high-frequency, high-speed induction machines is to open up the air gap until a magnetizing reactance in the range of 1 to 1 1/2 per unit is obtained. The larger air gap reduces zig-zag leakage and allows larger slot openings which in turn reduce slot leakage. A glance at Figure 2 will show that the power capabilities of an induction motor are changed very little when the magnetizing reactance is changed to 1.0 per unit from its usual value in the range of 2.0 per unit. The decreased magnetizing reactance makes the no-load and full-load motor currents of the same order of magnitude and requires more capacity for no-load excitation. However, the reduced leakage reactance

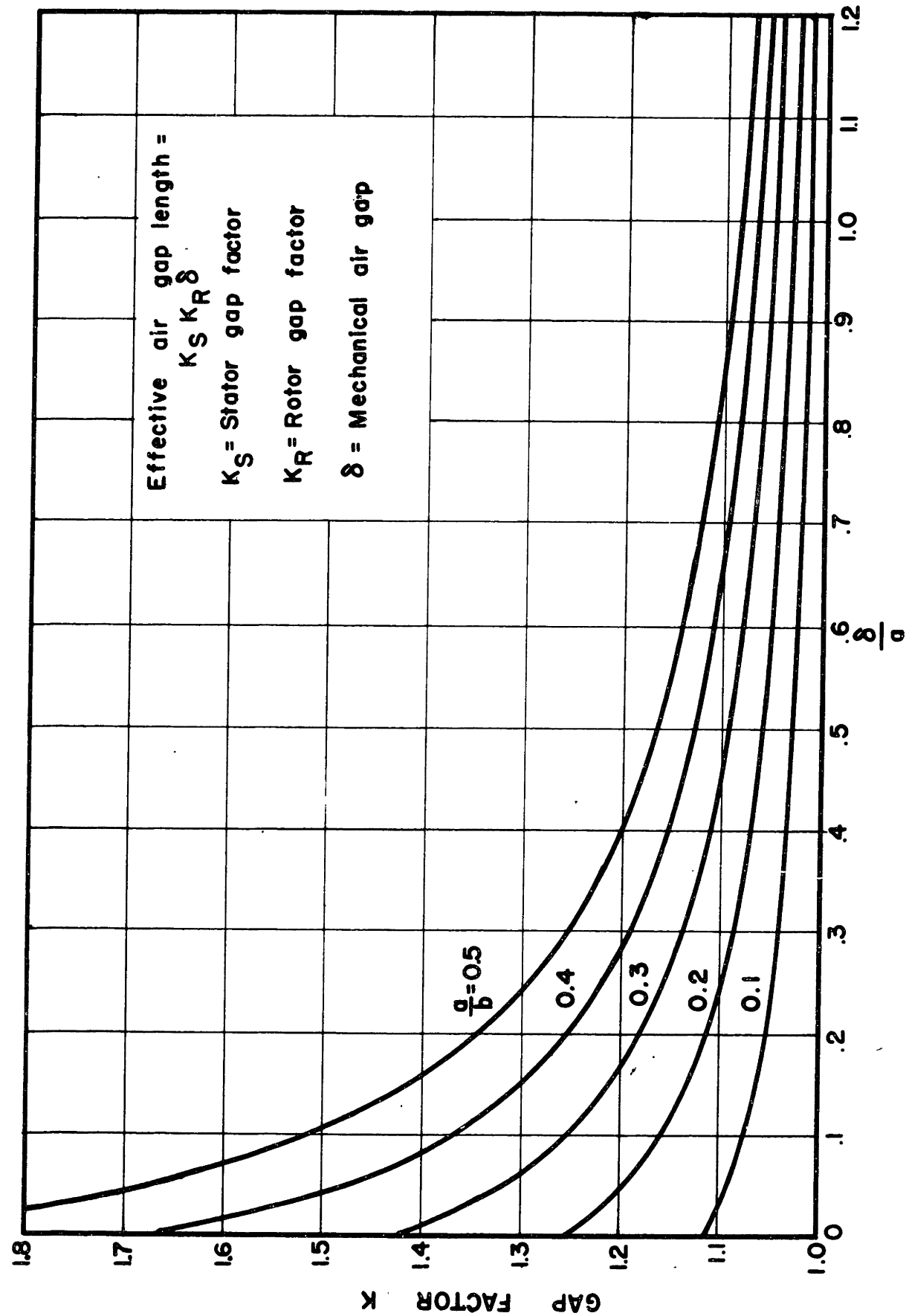

Fig 5 Gap factor for various values of slot opening and gap length.

produces a higher internal power peak and better inherent voltage regulation at a reduced volume.

The larger air gap also presents attractive mechanical qualities. Problems of alignment and concentricity which become increasingly important at high rotational speeds are simplified with a larger gap. Windage losses are reduced because of the lower velocity gradient in the air gap.

There is a limit to how much volume can be gained by decreasing the magnetizing reactance. This limit is set by the end-turn, belt, and skew leakage reactances whose permeances cannot be decreased as a result of increases in air-gap length. The optimum point for this design approach occurs when the sum of these three leakage reactances equals the sum of slot and zig-zag leakage reactances. This condition was approximately satisfied for the machine that was designed.

V

DESCRIPTION OF THE 60,000 RPM INDUCTION MACHINE

Using some of the principles and techniques outlined in the previous sections, the author designed a 60,000 rpm induction machine to meet the requirements outlined in the introduction. The punching of laminations and other mechanical construction was done by the Electroproducts Company of Waltham, Massachusetts. The stator was wound by the author. A two-pole, two-phase design was used which set the frequency at 1,000 cps for a rotational speed of 60,000 rpm. The overall machine dimensions are approximately 4 inches in diameter and 4 inches in length. The various parts of the alternator are shown in Figure 6. The stator stack has a length of 1 1/2 inches and and inside diameter of 1 1/2 inches. The squirrel cage rotor is 1 7/16 inches in diameter and 2 1/16 inches long (including end rings).

To some extent the design had to be a compromise between motor and alternator operation. In the former, a larger value of rotor resistance is desirable to provide sufficient starting torque and a rapid run-up time at high frequencies, whereas in the latter, a small rotor resistance minimizes the frequency changes with load for a constant rotational speed. The finished machine has a calculated starting torque of 27 per cent and a maximum torque of 250 per cent of full-load alternator torque for rated voltage and frequency. Maximum torque as a motor occurs at a slip of 5 per cent and full-load alternator output at a slip of -1 per cent. In

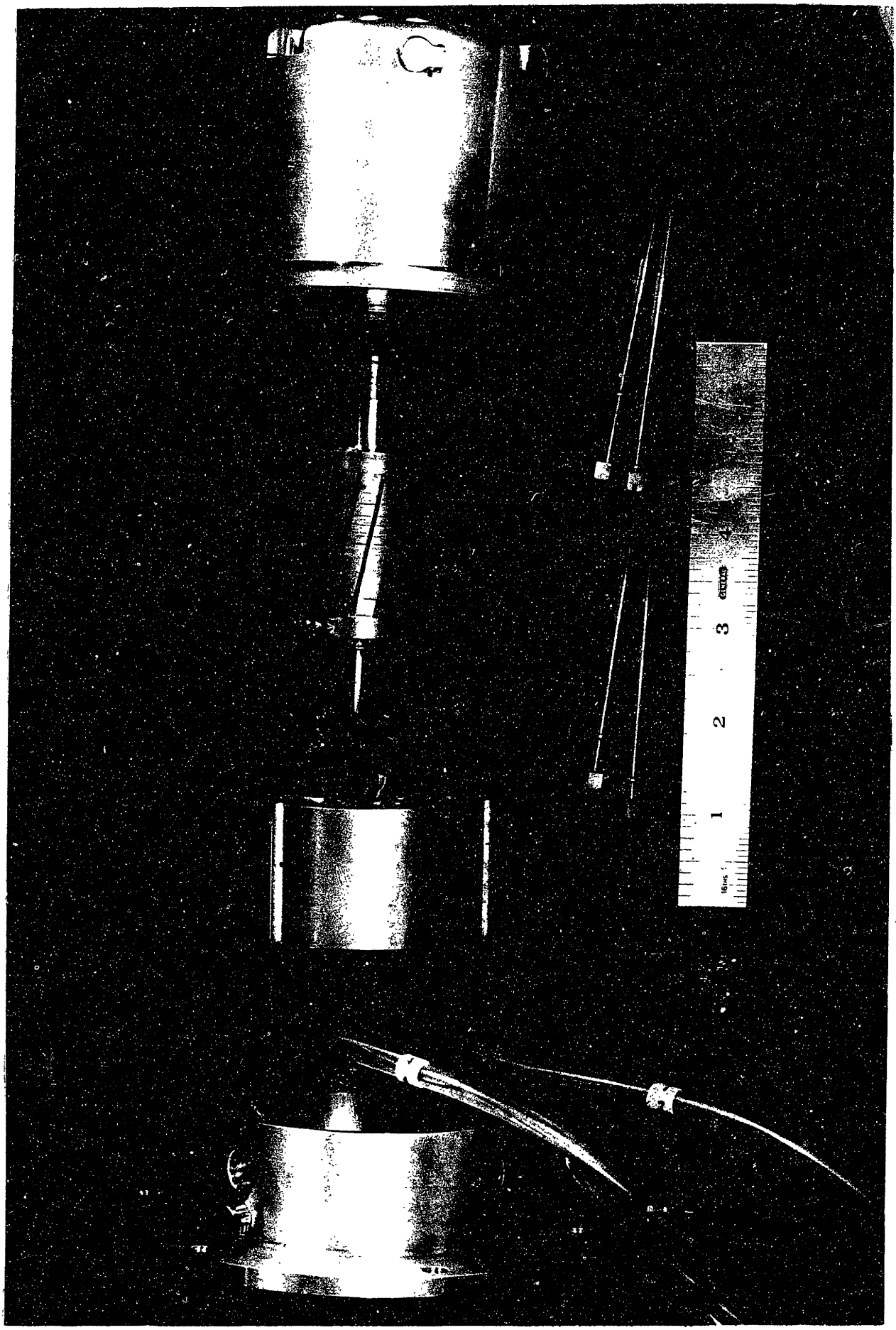

Fig 6 Exploded view of the 60,000 rpm induction machine

motor tests that were conducted, the starting torque proved to be sufficient. Because the rotor resistance can be easily increased by machining material from the end rings, the rings were purposely made large to allow good frequency regulation and an acceptable value of starting torque.

The maximum rotational stresses in the rotor laminations and end rings are approximately 20,000 pounds/inch^2 and 17,000 pounds/inch^2 respectively. Counterbore-type ball bearings with phenolic retainers are used in the machine. The stator and rotor laminations are bonded, and the rotor stack is keyed to the shaft with a Woodruff Key. The rotor was dynamically balanced in the Instrumentation Laboratory at M.I.T. Figure 7 shows an assembly drawing of the induction machine and drawings of the stator and rotor laminations are shown in Figure 8.

To reduce the excitation current and size of excitation capacitors, the output voltage of an induction generator should be as high as possible. Unfortunately, voltage in the range of 300 to 500 volts presented a distribution problem in the particular application for which the machine was designed. To resolve this situation, a transformer was incorporated in the stator of the machine with an excitation winding for 400 volts and a load winding of 150 volts. This resulted in a 40 per cent increase in copper section because the load and excitation currents did not add vectorially. However, when balanced against the alternate procedures of larger capacitors with higher current ratings or a transformer external to the machine, the 40 per cent increase in copper section did not look unattractive. The actual full-load generator ratings at 1000 cps and 60,000 rpm are as follows:

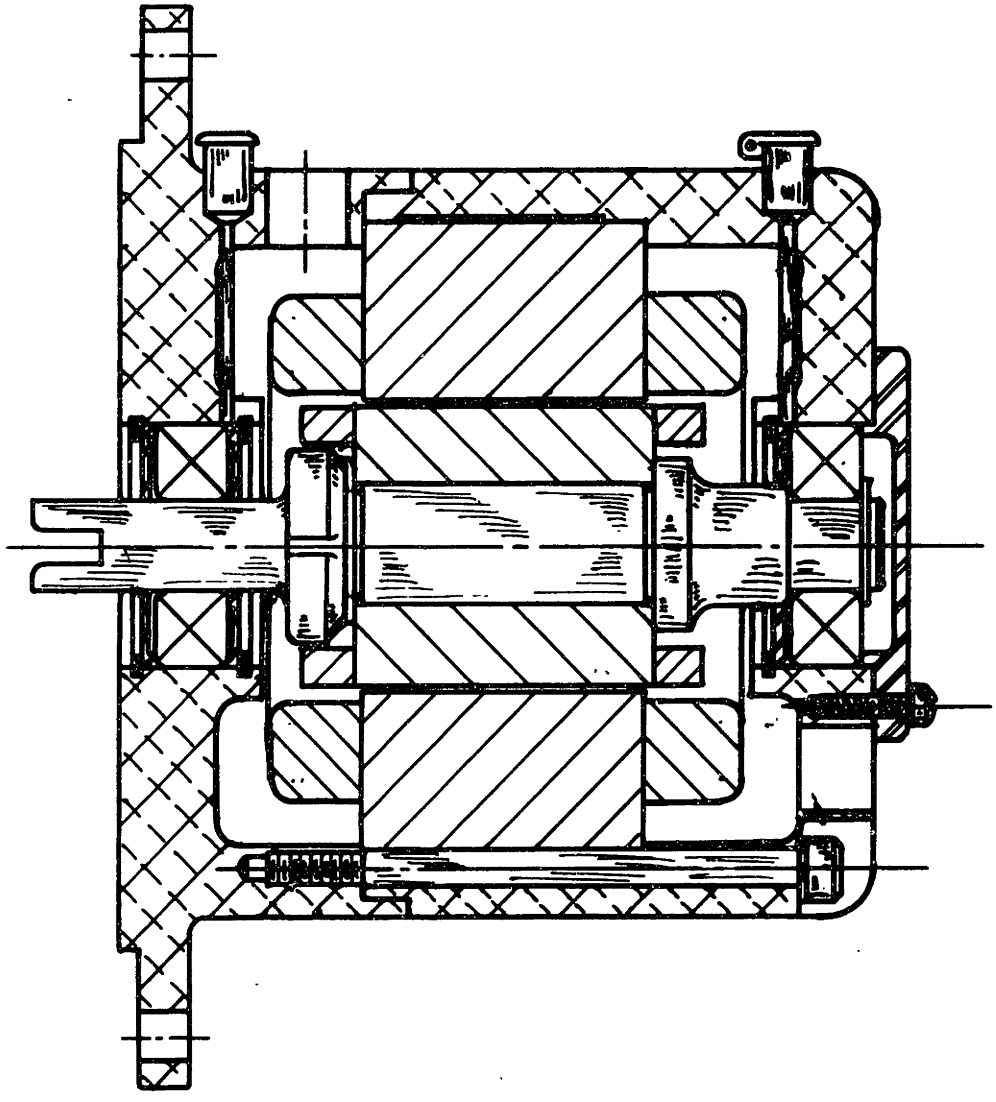

Fig 7 Assembly drawing of the induction machine.

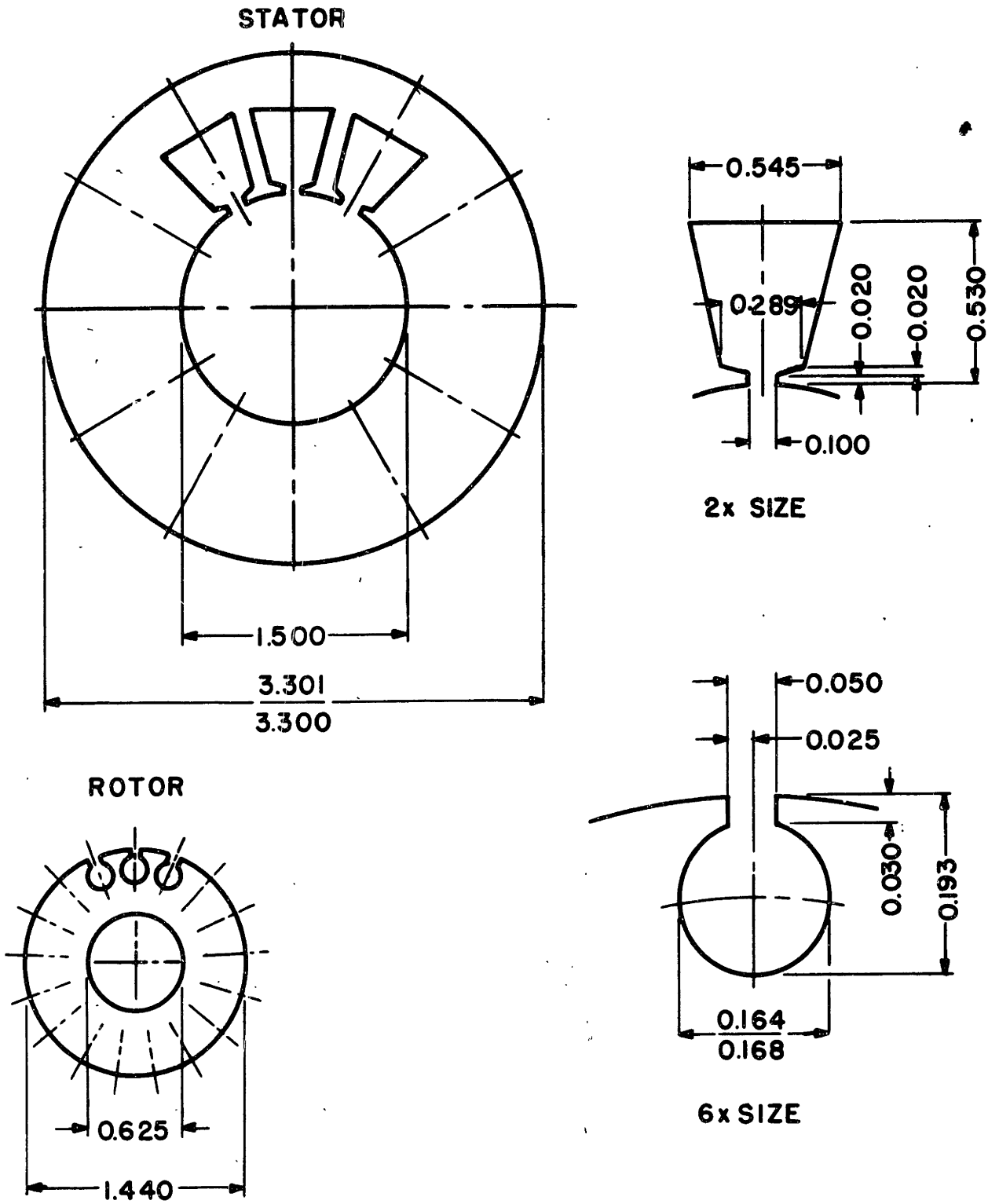

Fig 8 Drawing of the stator and rotor laminations of the induction machine

Load Winding (two-phase) At Unity Power Factor

Voltage 150 volts/phase

Current 4 amperes/phase

Excitation Winding (two-phase)

Voltage 400 volts/phase

Current 1 1/2 amperes/phase

Excitation Capacitance 0.6 microfarads/phase

A combination of 12 stator slots and 17 rotor slots was used in the design. This combination checked all right with the rules listed in W. R. Appleman's paper, "The Cause and Elimination of Noise in Small Motors", for quiet motor operation without locking or low-torque points at starting. To eliminate three of the four principle modes of vibration of the teeth due to magnetic forces at the gap, the rotor slots were skewed one stator-slot pitch as recommended in S. J. Mikina's article, "Effect of Skewing and Pole Spacing on Magnetic Noise in Electrical Machinery".

Although many designers favor a 5/6 pitch with 6 slots/pole, a 2/3 pitch was used to reduce the bulk of the end turns. A 2/3 pitch makes the third harmonic component of the air-gap flux wave equal to zero, but does not have the low harmonic pitch and distribution factors at higher harmonics. However, it was reasoned that the excitation capacitor would remove higher harmonics than the third. Even with the 2/3 pitch, there was insufficient space in the machine as first constructed to accommodate the end turns; and material had to be removed from the aluminum end bells. The lack of experience of the author in winding machines was probably the primary reason that additional end-turn space was required.

The actual details of the stator and rotor winding are listed below:

Stator: slot pitch - slots 1 and 5

wire sizes - 400 volt winding - No. 24 copper wire with formex and glass varnish insulation

- 150 volt winding - No. 21 copper wire with teflon insulation

coils/phase - 6 for each winding

series turns/coil - 400 volt winding - 42

150 volt winding - 16

series turns/phase - 400 volt winding - 252

150 volt winding - 96

winding factor - k_p = pitch factor = 0.866

k_d = distribution factor = 0.912

$k_w = k_p k_d = 0.790$

Rotor: squirrel cage winding

wire size - No. 6 bare copper wire

end ring - machined copper with an area of 0.05 $inch^2$

skew - one stator slot pitch (0.393 inches)

In order to allow for testing time in excess of the required operating period and to meet the motoring requirement, the machine was designed with relatively conservative core losses and current densities. The average stator core loss at rated voltage and frequency is 20 watts/pound. USS Transformer No. 72, 14 mil laminations with an insulating coating were used for both the stator and rotor stacks. The choice of gage size and silicon content was a compromise between the availability and higher punching rejection rates of thin high-silicon steels and the larger core

losses of thick low-silicon laminations. The following table summarizes the magnetic circuit and core loss aspects of the machine. The calculations are in accordance with the methods outlined in Kuhlmann's design text. The high frequency rotor tooth-tip core loss was estimated from an equation in the "Induction Motor Design Notes" of Roger B. Bross of the M.I.T. Instrumentation Laboratory.

CALCULATED FLUX DENSITY AND CORE LOSS AT RATED VOLTAGE AND FREQUENCY

	Density (kilolines/in^2)	MMF (ampere-turns)	Core Loss (watts)	Weight (pounds)
Stator Core	45	6	23	1.3
Stator Teeth	69	5	13	0.3
Rotor Core	69	4	negligible	0.2
Rotor Teeth	57	1	12	0.1
Air Gap	18	201	—	---
		Total	48 watts	

Full-load current densities are 6300 amperes/inch^2 in the load winding and 4700 amperes/inch^2 in the excitation winding. The lower design density in the excitation winding is to allow for excitation currents in the range of 2.0 to 2.5 amperes without serious overheating when the alternator is tested without the benefit of external control circuits to supplement the small amount of non-linearity embodied in the machine. The saturation factor under rated operating conditions is 1.08.

In the design particular emphasis was placed upon minimizing and balancing leakage reactance. The large-air-gap approach discussed in

Section IV was followed, and the air gap was increased to 0.03 inches. For this value of air gap and the air-gap geometry shown in Figure 8, the value of $\frac{K_{zz}}{\delta}$ from Figure 4 is about 3.3. The relative slot permeance contributed by the slot openings is $\frac{0.020}{0.100} = 0.20$ for the stator slots and $\frac{0.30}{0.50} = 0.60$ for the rotor slots. To produce balanced stator leakage reactances and resistances for the two phases, care was taken to put the same number of coil sides for each phase in the bottoms of the slots. Since the stator was random wound, only half of each phase could be wound at a time to meet the balancing requirement. The detailed winding layout and random winding instructions that were followed are presented in the Appendix.

The larger air gap resulted in a magnetizing reactance of 1.18 per unit and the values of leakage reactance listed below. Belt and skew leakage reactances were calculated from equations in R. B. Bross's Design Notes and then put on a normalized basis. Slot, zig-zag, and end turn leakage reactances were computed from equations (7), (8) and (9).

Slot leakage reactance -	0.055 per unit
Zig-zag leakage reactance -	0.034 per unit
End turn leakage reactance -	0.041 per unit
Belt leakage reactance -	0.008 per unit
Skew leakage reactance -	0.025 per unit
Total leakage reactance	0.163 per unit

VI

STEADY-STATE EQUIVALENT CIRCUIT OF THE 60,000 RPM INDUCTION GENERATOR

As in motor operation the equivalent circuit of an induction machine is a useful tool in the analysis of generator performance. Complete machine analysis must necessarily be based upon magnetization curves of the machine and torque-speed characteristics of the prime mover as well as the equivalent circuit. A complete analysis of an isolated induction generator is currently being investigated by Mr. W. T. Peake of the Electrical Engineering Department as a thesis study. Therefore, it is not the intention of the author to present a detailed analysis of the machine. However, a discussion of generator operation and an equivalent circuit for the particular machine which was built are subsequently presented.

The operation of a capacitor-excited-induction generator is in many ways analogous to a self-excited d-c shunt generator. The intersection of the capacitive-reactance line with a plot of no-load terminal volts versus terminal current can be used to determine the no-load generator voltage of an induction generator in much the same manner as the intersection of the field-resistance line and the magnetization curve of a d-c machine are used. The initial build up of voltage in an induction generator is caused by residual flux in the rotor laminations in a manner analogous to the way the residual magnetism of the stator structure initiates voltage build up in a self-excited d-c machine. The induction

generator acts unstably when the capacitive-reactance and air-gap lines coincide with a constant-speed prime mover just as the d-c machine exhibits unstable operation when the field-resistance line coincides with the linear portion of the magnetization curve. However, the induction generator can be made to operate on the air-gap line in an analogous fashion to the d-c rototrol. This fact was demonstrated by the author in experimental work conducted in the Electrical Machinery Laboratory in which adjustable iron core reactances were placed in series with the excitation capacitors of a three phase isolated induction generator as shown in Figure 9. The iron core reactors supplied sufficient non-linearity to allow stabilized operation under load at output voltages of 10 and 20 per cent of rated voltage. Since a larger value of capacitive reactance was needed to compensate for the additional inductive reactance, a smaller value of excitation capacitor was required. A disadvantage of this system is that capacitor voltage is greater than terminal voltage by the amount of voltage across the reactor.

The basic equivalent circuit for an induction generator is shown in Figure 10. The circuit is on a line-to-neutral basis and all quantities are per phase. The slip which is normally defined as $\frac{\omega_1 - \omega_n}{\omega_1}$ for motor operation is negative for generator operation because shaft speed ω_n is greater than stator angular frequency ω_1. In Figure 10 s is defined as a positive quantity equal to $\frac{\omega_n - \omega_1}{\omega_1}$ which makes a +s in the motor equivalent circuit become a -s in the generator circuit. The symbols r_1 and r_2 represent the stator and rotor resistance respectively and ℓ_1 and ℓ_2 the stator and rotor leakage inductances. The magnetizing inductance is ℓ_m and the core-loss resistance is r_m.

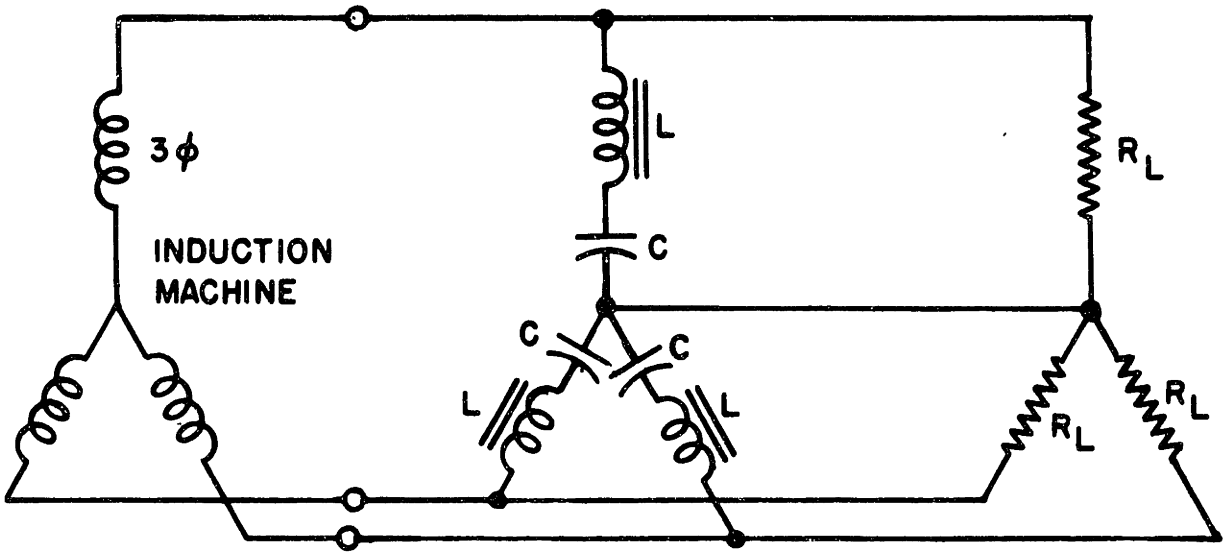

Fig 9 Circuit for operation of an induction generator on the air gap line.

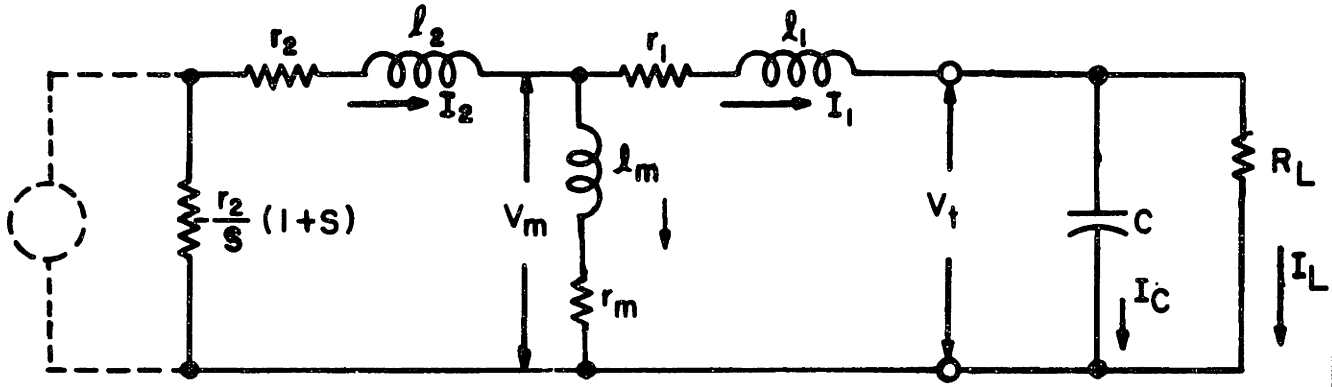

Fig 10 Basic equivalent circuit of induction generator.

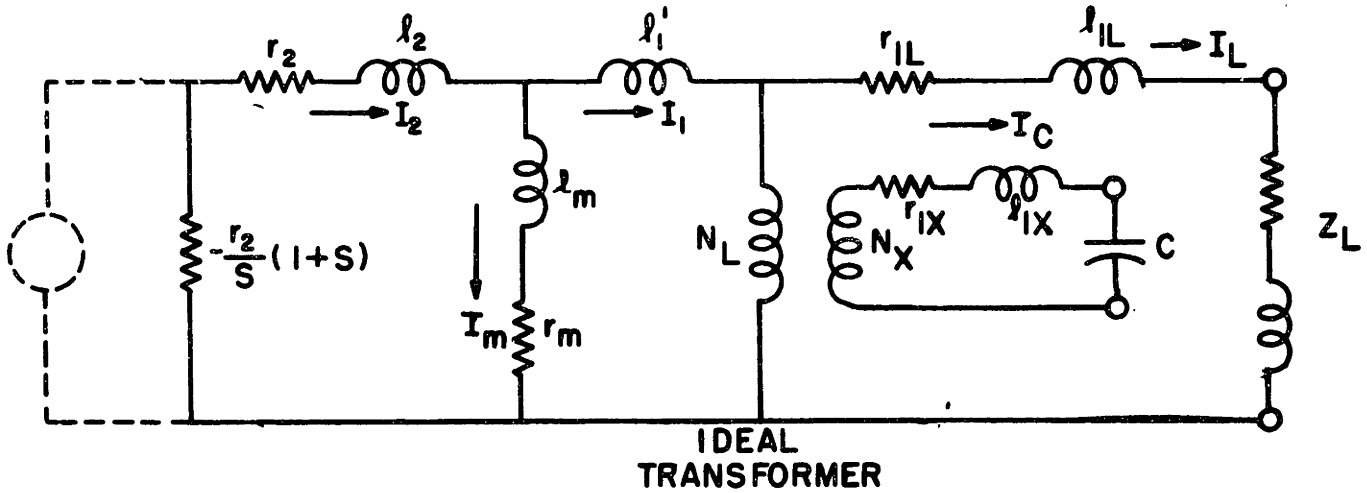

Fig. 11 Equivalent circuit of the 60,000 r pm induction generator.

For steady operation a power and reactive power balance must be satisfied by the machine and external circuit. These balances are stated symbolically in the following equations:

$$\frac{r_2}{s}(1+s)I_2^2 = r_2I_2^2 + r_1I_1^2 + r_mI_m^2 + R_LI_L^2 \qquad (16)$$

$$\frac{1}{\omega_1 C} I_C^2 = \omega_1 \ell_1 I_1^2 + \omega_1 \ell_2 I_2^2 + \omega_1 \ell_m I_m^2 \qquad (17)$$

Stated in words the equations say that the mechanical input power less friction and windage equals the sum of the losses and output electrical power, and that the lagging reactive power supplied by the capacitor equals the total reactive power required to produce the leakage and magnetizing fluxes. Plots of V_M versus I_M for various values of ω_1 and prime-mover torque-speed curves are necessary for the determination of terminal voltage and frequency for a certain combination of C and R_L.

The equivalent circuit for the 60,000 rpm machine is complicated somewhat by the presence of the transformer coupling between the load and excitation windings. The equivalent circuit for one phase shown in Figure 11 was deduced after a study of the leakage flux paths described by P. L. Alger in his book "The Nature of Polyphase Induction Machines".

The quantities appearing in the circuit of Figure 11 are defined as follows:

Z_L = the load impedance

r_{1L} = the resistance of the load (150 volt) winding

ℓ_{1L} = the stator slot leakage inductance of the load winding + 1/2(end turn leakage inductance of the load winding)

C = the excitation capacitance

r_{1x} = the resistance of the excitation (400 volt) winding

ℓ_{1x} = the stator slot leakage inductance of the excitation winding + 1/2(end turn leakage inductance of the excitation winding)

N_L = the series turns/phase in the load winding

N_x = the series turns/phase in the excitation winding

ℓ_1' = 1/2(zig-zag leakage inductance + skew leakage inductance + belt leakage inductance) referred to the load winding

ℓ_m = the magnetizing inductance referred to the load winding

r_m = the core loss resistance referred to the load winding

ℓ_2 = 1/2(zig-zag leakage inductance + skew leakage inductance + belt leakage inductance + end turn leakage inductance) referred to the load winding + the rotor slot leakage reactance referred to the load winding

r_2 = the rotor resistance referred to the load winding

$s = \frac{\omega_n - \omega_1}{\omega_1}$ where ω_n is the shaft speed in electrical radians/second (the same as mechanical radians for a 2 pole machine) and ω_1 is the angular frequency of stator currents

The numerical values of the machine parameters as calculated from design quantities are listed below. The calculations are explained in the Appendix.

Resistance values are in ohms and inductance values are in millihenries (10^{-3} henries).

$r_{1L} = 1.13$	$\ell_1' = 0.202$	$\ell_2 = 0.484$
$\ell_{1L} = 0.290$	$\ell_m = 6.97$	$N_L = 96$ turns/phase
$r_{1x} = 5.96$	$r_m = 2.36$	$N_x = 252$ turns/phase
$\ell_{1x} = 2.00$	$r_2 = 0.319$	

The magnetizing inductance ℓ_m is calculated for a value of machine flux corresponding to rated voltage (150 volts) across the series combination of r_m and ℓ_m. The saturation factor for this condition is 1.08. Listed below are magnetizing inductances and saturation factors calculated from the magnetic circuit for fluxes corresponding to various values of excitation voltage (voltage across the series combination of ℓ_m and r_m).

Excitation Voltage (volts)	Saturation Factor	ℓ_m (millihenries)
112 $(\frac{f}{1000})$	1.070	7.02
150 $(\frac{f}{1000})$	1.078	6.97
187 $(\frac{f}{1000})$	1.102	6.81
225 $(\frac{f}{1000})$	1.195	6.29

VII

TESTS OF THE 60,000 RPM MACHINE AS A MOTOR

Motor tests were separated into two parts. The first set of tests was standard blocked-rotor and no-load induction-motor tests performed in the Electrical Machinery and Dynamic Analysis and Control Laboratories, and the second was load tests performed in the Gas Turbine Laboratory.

Standard Blocked-Rotor and No-Load Tests

The table below compares experimental values of leakage and magnetizing inductances measured in the conventional blocked-rotor and no-load tests at 60 cps and 400 cps with values calculated from design quantities. At each frequency the 2 phase voltage source was fed through variacs to reduce the voltage applied to the machine. To prevent excessive magnetizing current in the no-load tests at low frequencies, the applied voltage was less than $\frac{f}{1000}$ of the rated value at 1000 cps. The blocked-rotor current was kept at or below the rated value. The complete data from which the measured values were computed is included in the Appendix.

	Measured at 60 cps (millihenries)	Measured at 400 cps (millihenries)	Calculated from Design (millihenries)
Total Leakage Inductance (400 volt winding)	6.4	7.9	6.8
Total Leakage Inductance (150 volt winding)	0.86	0.98	0.92
Magnetizing Inductance (400 volt winding)	48.5	48.5	48.1

Although there is not exact agreement between measured and calculated values, particularly in the case of the leakage inductances, the results are sufficiently close to indicate that classical-design formulas for rotating machines can be applied in the design of small high-frequency machines. It appears from the data that leakage inductance increases with frequency. Actually this conclusion cannot be safely made because the leakage reactance at 60 cps is much smaller than the resistance and is found by taking the square root of the difference of squares of two quantities that are almost equal, and because measuring instruments with a guaranteed accuracy to only 133 cps had to be used in the 400 cps test.

Immediately upon completion of the blocked-rotor and no-load tests performed at 60 cps in the Electrical Machinery Laboratory, the d-c resistances of the stator windings were measured on the Wheatstone bridge in the Measurements Laboratory. The measured resistance values are compared below with values calculated for a temperature of 75 degrees Centigrade.

	Measured (ohms)	Calculated (ohms)
Phase 1 - 400 volt winding	5.34	5.96
150 volt winding	1.02	1.13
Phase 2 - 400 volt winding	5.48	5.96
150 volt winding	1.09	1.13

The results indicate that the machine winding temperatures were probably less than 75 degrees Centigrade when the measurements were taken.

An eddy-current calculation, performed as outlined in Section III, indicated that the eddy-current effect in the stator windings is negligible

at 60 cps and 400 cps. This fact means that the stator resistance can be taken equal to the d-c value without significant error, and that rotor resistance can be estimated closely from the blocked-rotor data. If this procedure is followed, the following results are obtained:

	Measured 60 cps (ohms)	Measured 400 cps (ohms)	Calculated from Design D-C at 75°C (ohms)
r_2 referred to 400 volt winding	1.76	3.23	2.20
r_2 referred to 150 volt winding	0.270	0.53	0.32

These results indicate two things. First, the fact that the 60 cps values are both about 20 per cent less than the calculated values at 75 degrees Centigrade shows that the winding temperatures did not rise much above room temperature during the blocked-rotor tests at 60 cps. Second, and certainly more interesting, the increased rotor resistance at 400 cps shows that the eddy-current effect in the rotor can be an important factor at large values of slip in high frequency induction motors. With the fractional increase in resistance proportional to the fourth power of the conductor thickness, it is not difficult to see how rotor bar resistances 1 1/2 to 2 times the d-c value are possible at starting. A complete analysis of the eddy-current effect for rectangular bars is carried out by P. L. Alger in his book, "The Nature of Polyphase Induction Machines". To the designer the increased rotor resistance at starting means a higher starting torque, but it may also mean a minimum in the torque-speed curve between the starting and maximum torque points. This latter condition

can come about because the fractional increase in bar resistance is also proportional to the square of rotor frequency which decreases as the motor comes up to speed.

To measure the friction and windage losses in the machine, no-load runs were made at 60 cps and 400 cps at reduced voltages which made core loss negligible but which did not cause an appreciable decrease in operating speed. After the stator I^2R losses were subtracted from the input power readings, friction and windage losses of 2 watts at 3600 rpm and 14 watts at 24,000 rpm remained. These low friction and windage losses are partly due to the low-friction forces of ball bearings, but are also a result of the large air gap in the machine.

Load Tests

Figure 12 shows the induction machine mounted to drive an air-absorption-type dynamometer in the Gas Turbine Laboratory. The dynamometer was designed and developed at the Dynamic Analysis and Control Laboratory. Two-phase power for the induction machine was obtained from the output of an improvised Scott transformer set-up which was supplied by the 3-phase variable frequency alternator in the wind tunnel. The complete circuit diagram is shown in Figure 13. An oscilloscope was used to check the phase angle at the output of the Scott transformer. A variac was required in each phase because the transformers did not have an 0.866 tap and the two transformer output voltages normally differed by about 10 per cent in magnitude. Throughout the tests the pattern on the oscilloscope remained circular indicating a 90 degree phase angle. Voltage was applied to the 400 volt windings because the

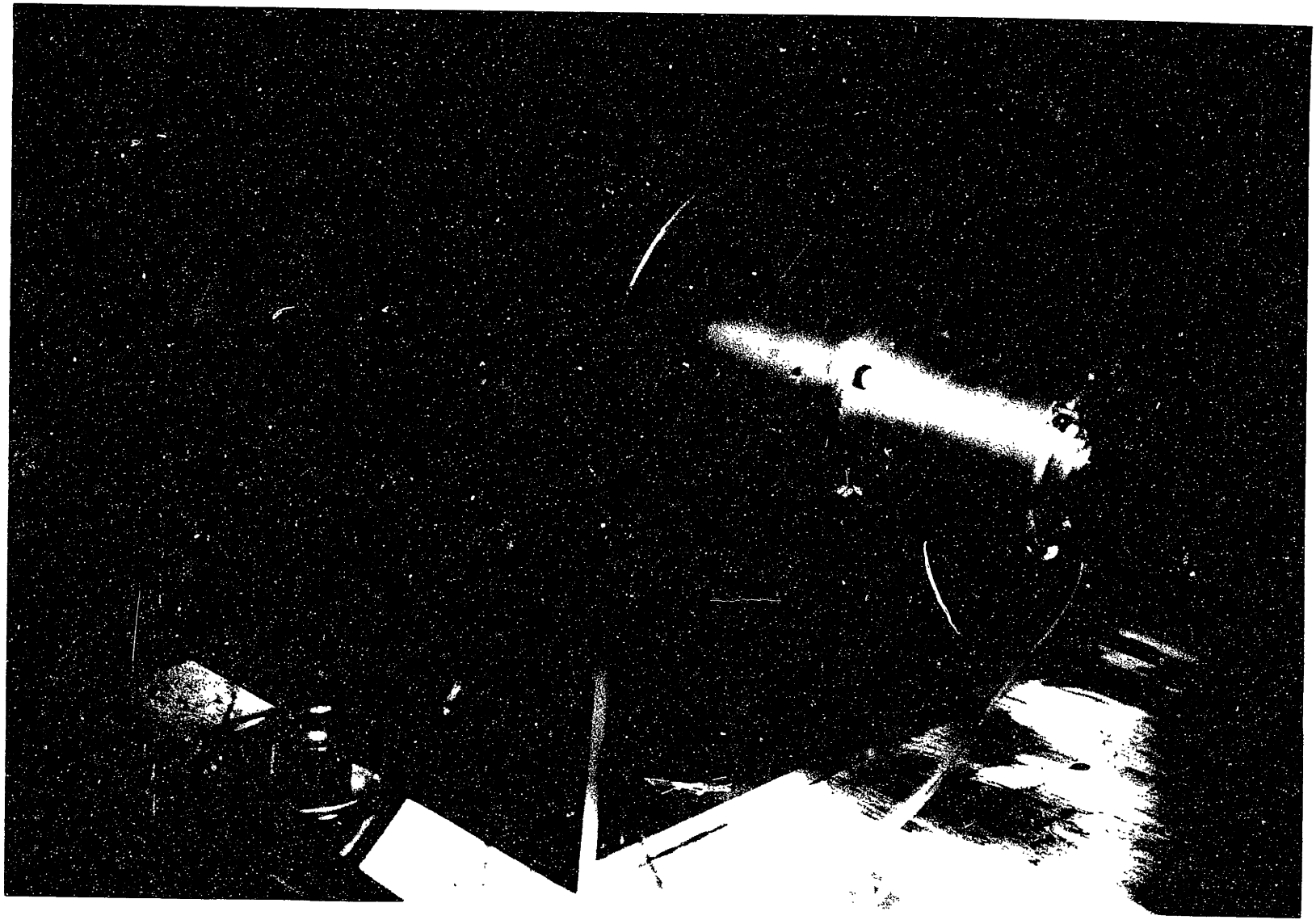

Fig 12 Induction machine mounted to drive an air-absorption-type dynamometer

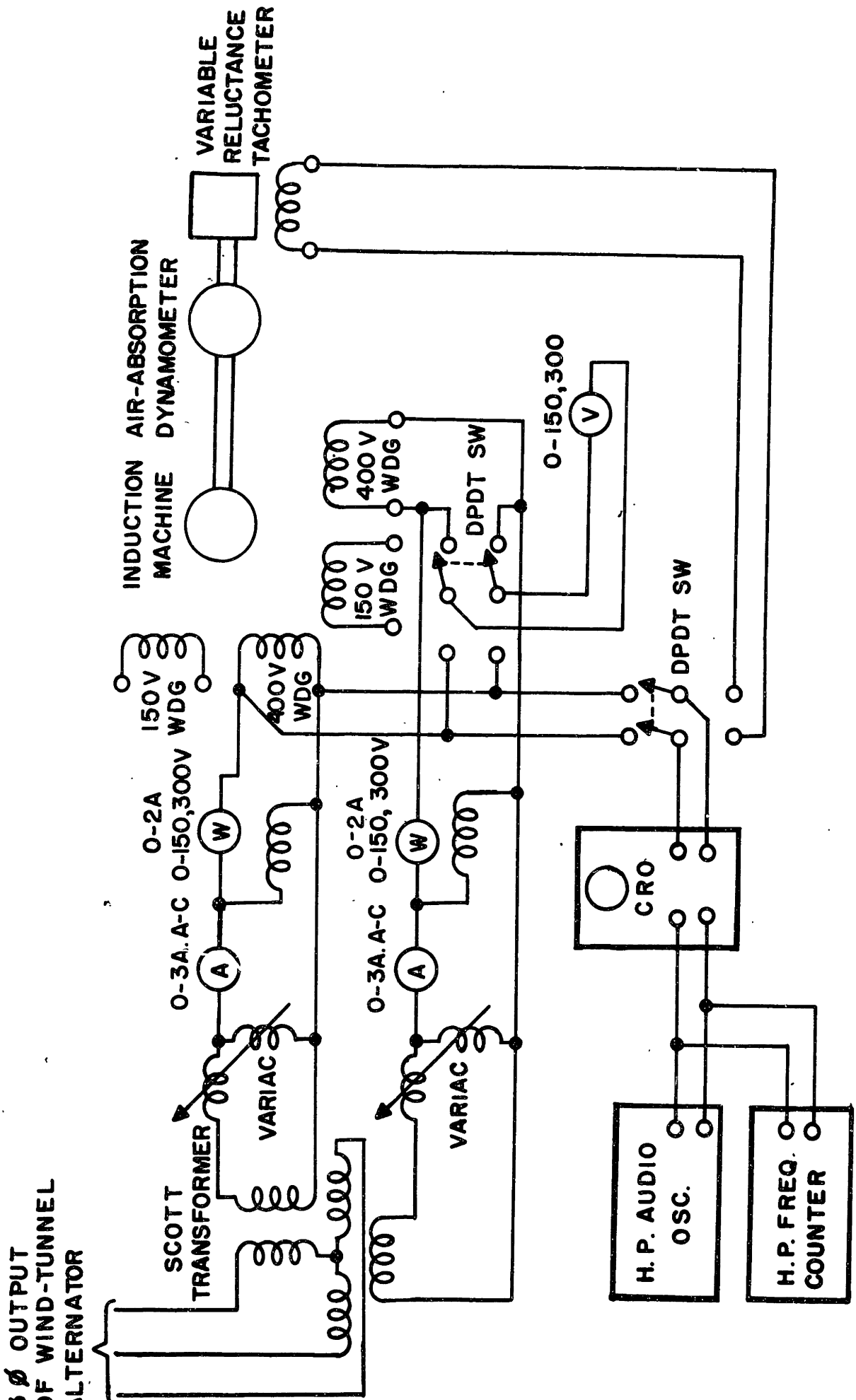

Fig. 13 Connection diagram for motor load tests

range of voltages required for this winding at the lower frequencies was convenient to work with. Also lower currents were required for the high voltage windings.

Speed was measured by comparing the output of a variable-reluctance-type tachometer with the output of a Hewlett-Packard audio oscillator by means of a lissajous pattern on an oscilloscope. The oscillator frequency was then determined to an accuracy of one cycle by a digital-type Hewlett-Packard frequency counter. Line frequency was measured in the same manner with phase voltage substituted for tachometer voltage through a switching arrangement shown in Figure 13.

The dynamometer is essentially an air pump with a built in heat exchanger. The load on the dynamometer is changed by varying the density of the input air. The outer housing is mounted on bearings so that the total input mechanical torque to the dynamometer is transmitted to the housing. The input water pipe for the heat exchanger also serves as a torsional spring for the dynamometer housing. A cantilever spring is also provided. The position of the dynamometer housing is measured by a sensitive reluctance-type pickup and actual housing deflections under load are very small. Load torques are measured by adding sufficient weights to a weight pan attached to the housing to return the housing to its initial no-load position.

The maximum output frequency of the variable-frequency power source was 400 cps. Runs at this frequency had to be limited to about 15 minutes because the bearings of the wind-tunnel motor-generator set overheated rapidly at shaft speeds corresponding to 400 cps. Torque data

taken at nominal stator frequencies of 200, 300 and 400 cps is included in the Appendix. All electrical quantities except the voltage readings were measured on meters with a guaranteed frequency response of 133 cps.

Figure 14 shows measured and calculated curves with a stator frequency of 206 cps. The calculated curve was computed from the equivalent circuit by the method outlined by C. G. Veinott in his paper, "Performance Calculations on Induction Motors". The calculations are included in the Appendix. The run was made with balanced 2 phase voltages of approximately 50 volts applied to the 400 volt windings. Fifty volts is 63 per cent of rated voltage for the 400 volt windings at 200 cps. It was found that a more stable operating technique for obtaining torque points in the vicinity of maximum torque was by a reduction in the applied voltage rather than by a change in dynamometer loading. The torque data was then corrected to 50 volts by the square of the voltage ratio. The measured and calculated curves show close agreement in the operating range. The discrepancy of the torque values in the range of slips from 0.3 to 0.6 probably represents a slight cusping effect due to slot openings.

In Figure 15 measured and calculated torque-slip curves for an applied voltage of 115 volts at 400 cps are plotted. This value of voltage is 72 per cent of rated voltage at 400 cps. The running time restrictions imposed by the supply generator did not allow sufficient time to obtain more points on the curve. The maximum disagreement between measured and calculated curves is about 15 per cent. The applied starting voltage for this run was 65 volts/phase or about 40 per cent.

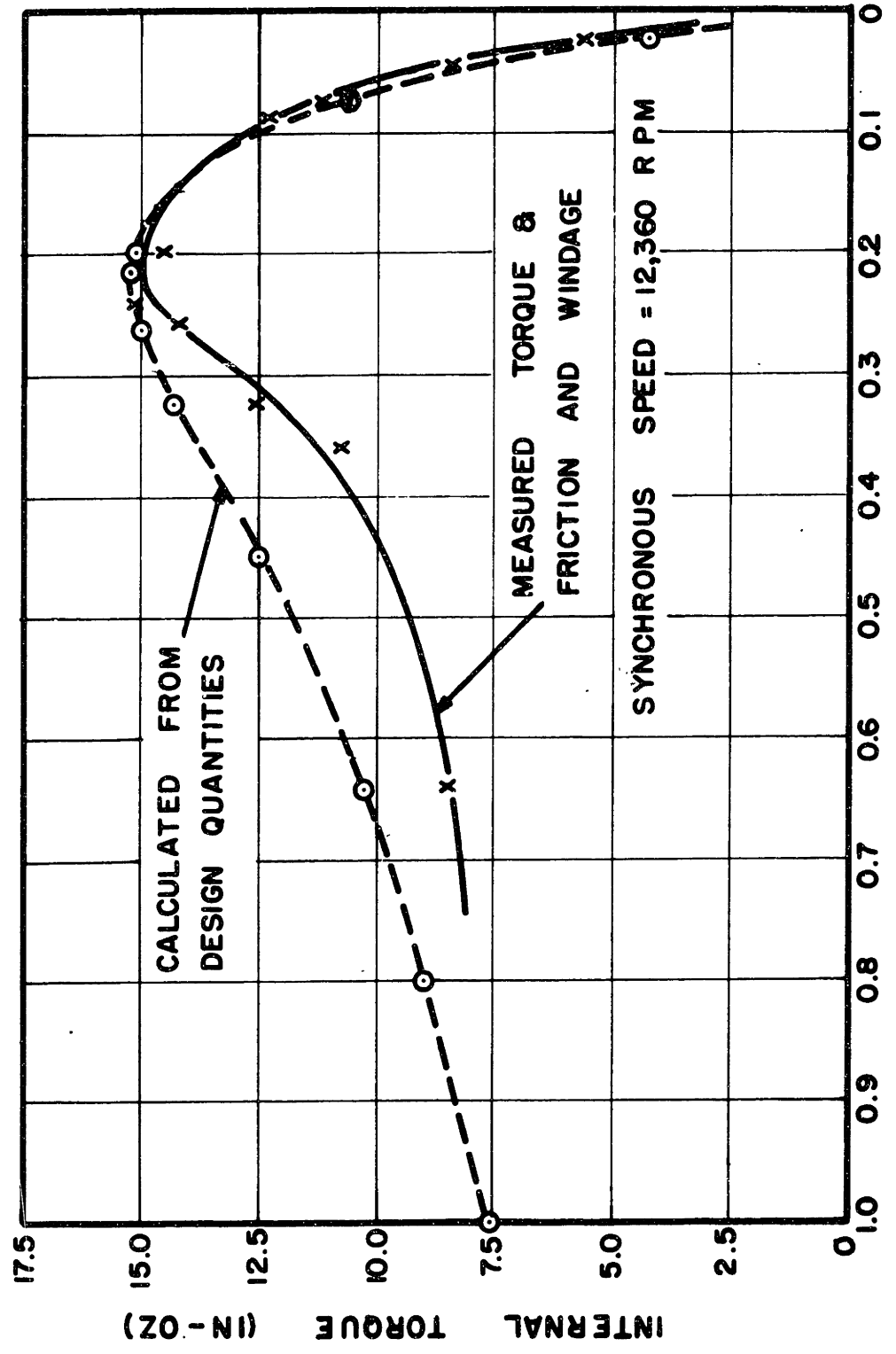

Fig. 14 Measure and calculated torque – slip curves at 206 cps.

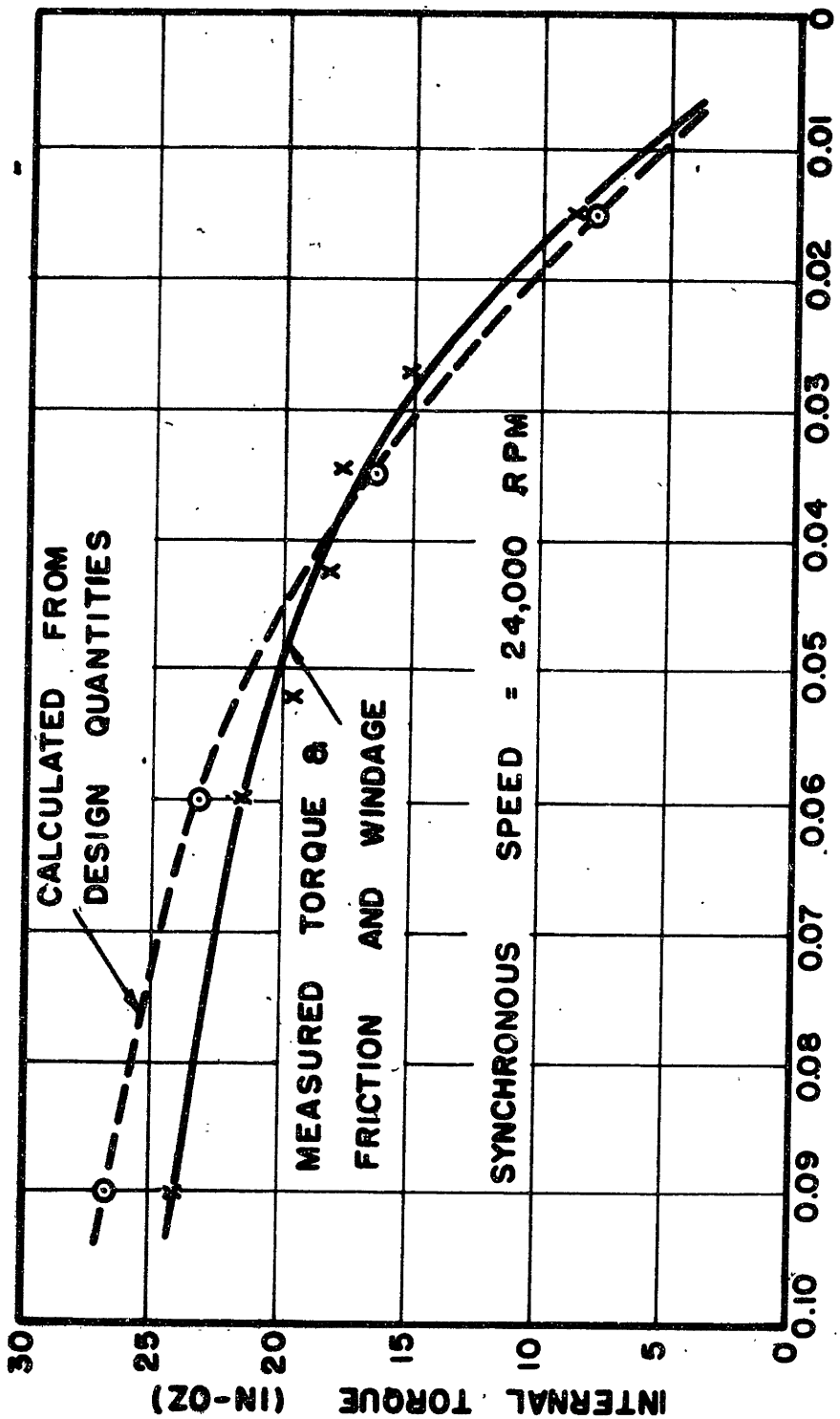

Fig. 15 Measured and calculated torque-slip curves at 400 cps.

The results of the load tests indicate, as do the results of the no-load and blocked-rotor tests, that classical design formulas and analytical techniques can be utilized in the design of small high speed machinery. Machine performance can be predicted by the designer with a fair degree of accuracy.

Although 1000 cps motor tests could not be performed at this time because a source was not available, the tests that were conducted indicate that satisfactory motor performance at frequencies higher than 400 cps can be expected. This fact is particularly demonstrated by the ability of the motor to come up to operating speed at 400 cps under a small dynamometer load with only 40 per cent voltage applied.

VIII

TESTS OF THE 60,000 RPM INDUCTION MACHINE AS AN ALTERNATOR

The induction machine was driven over a speed range of 18,000 rpm to 42,000 rpm by a single-nozzle air turbine in the Gas Turbine Laboratory. Runs at higher speeds were not made because the bearing lubricant started to burn off one of the turbine bearings at 42,000 rpm. Bearings of an improved type, currently on order, are to be installed in the turbine and induction machine.

The connection diagram is shown in Figure 16. Figure 17 shows the turbo-alternator rig and in Figure 18 the rig and some of the instrumentation are shown. Not shown in Figure 18 are the manometers used to measure various turbine pressures.

Various electrical loads were applied at output frequencies of 300, 400, 500, 600 and 700 cps. At the start of each run, an amount of capacity equal to the calculated value required for no-load excitation at the desired frequency was connected across each of the excitation windings. Turbine speed was gradually increased until voltage build-up was observed. Resistances were then connected to the load windings, and the machine was loaded electrically. Time for each run was limited to approximately 25 minutes because of heating caused by bearing friction and alternator losses. Shaft speed and frequency were measured in the same manner as described in the section on motor load tests.

Maximum electrical power at each frequency was a function of turbine limitations. Most of the runs were made at speeds other than the

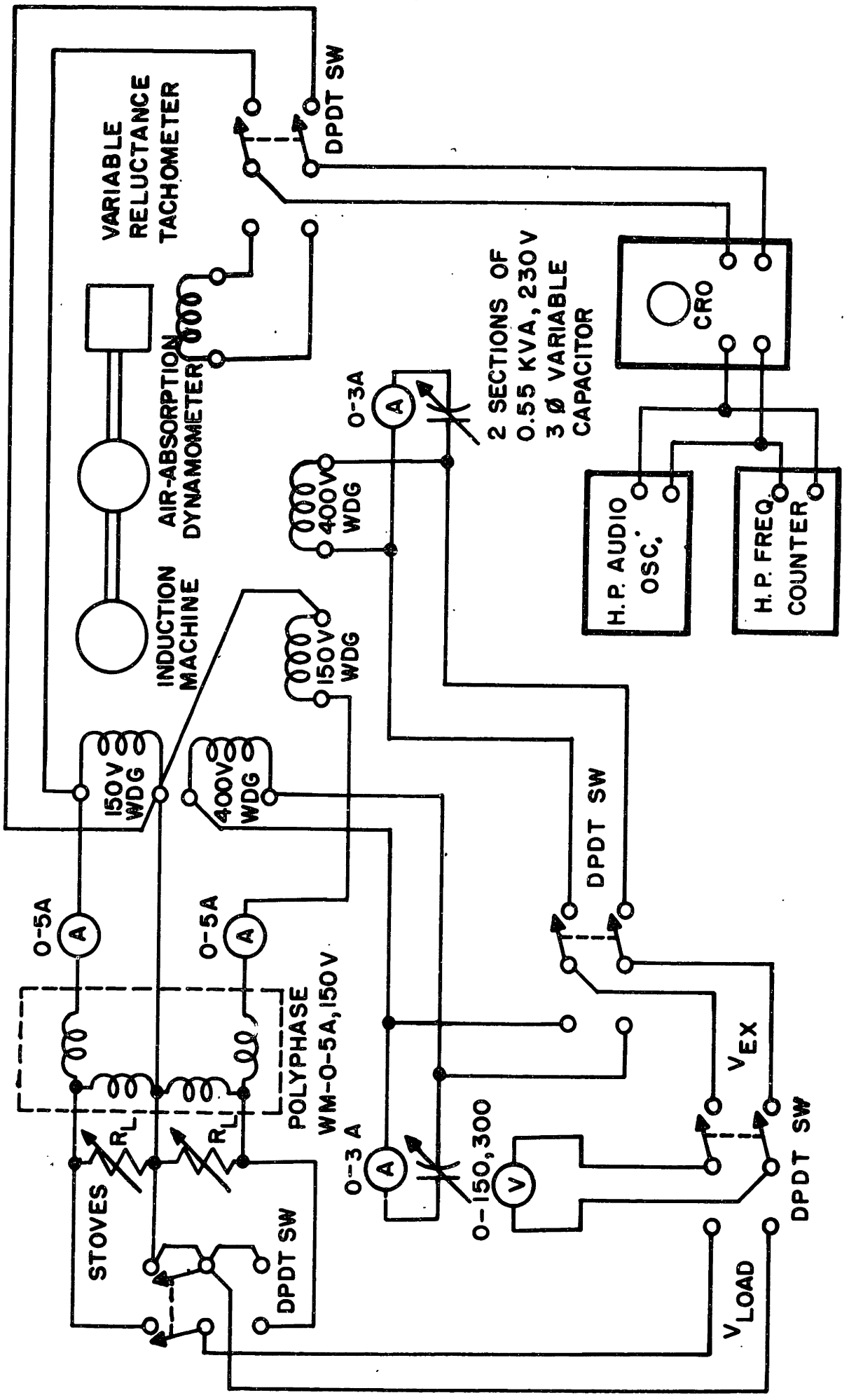

Fig. 16 Connection diagram for alternator tests

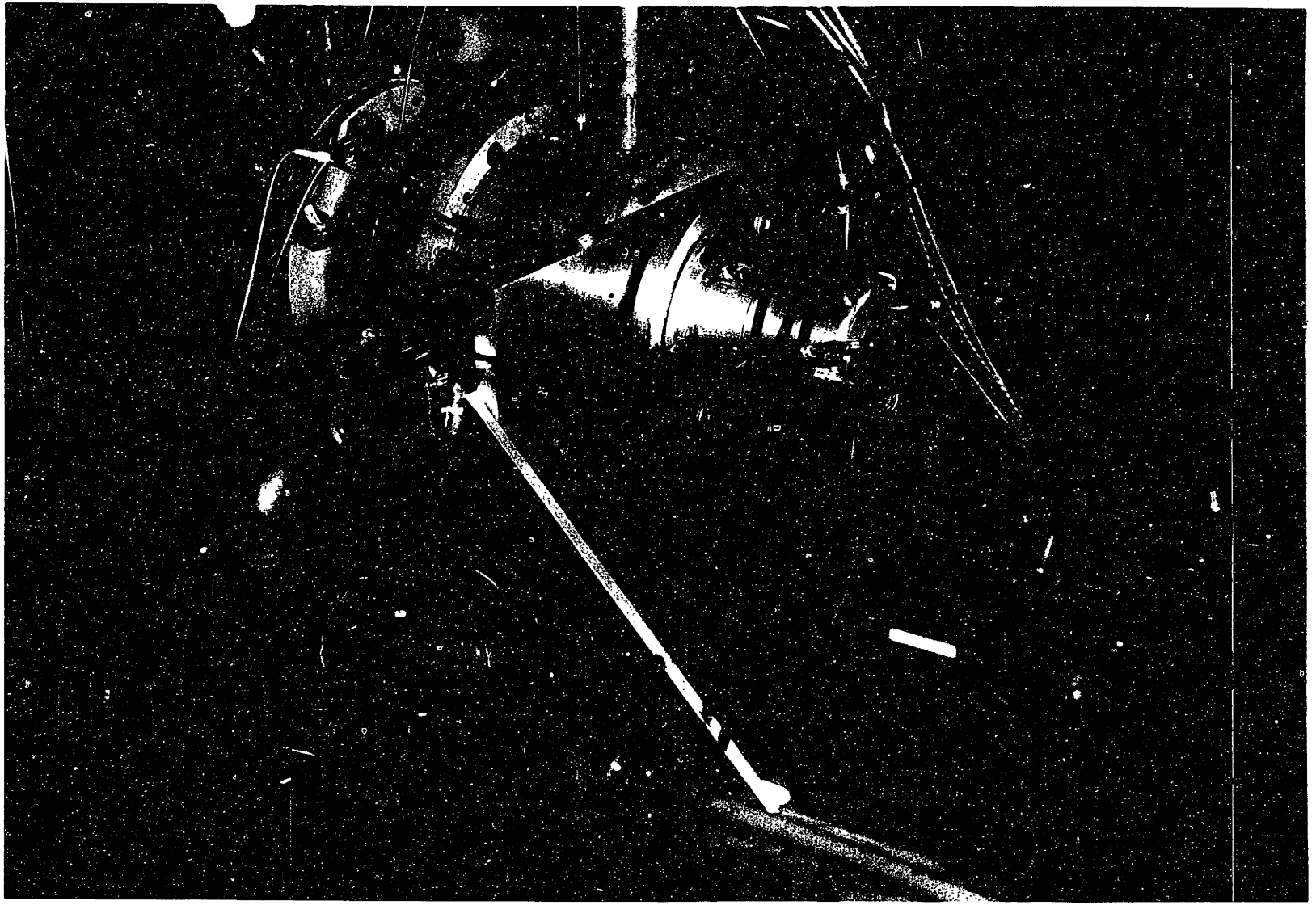

Fig 17 Turbo-alternator rig

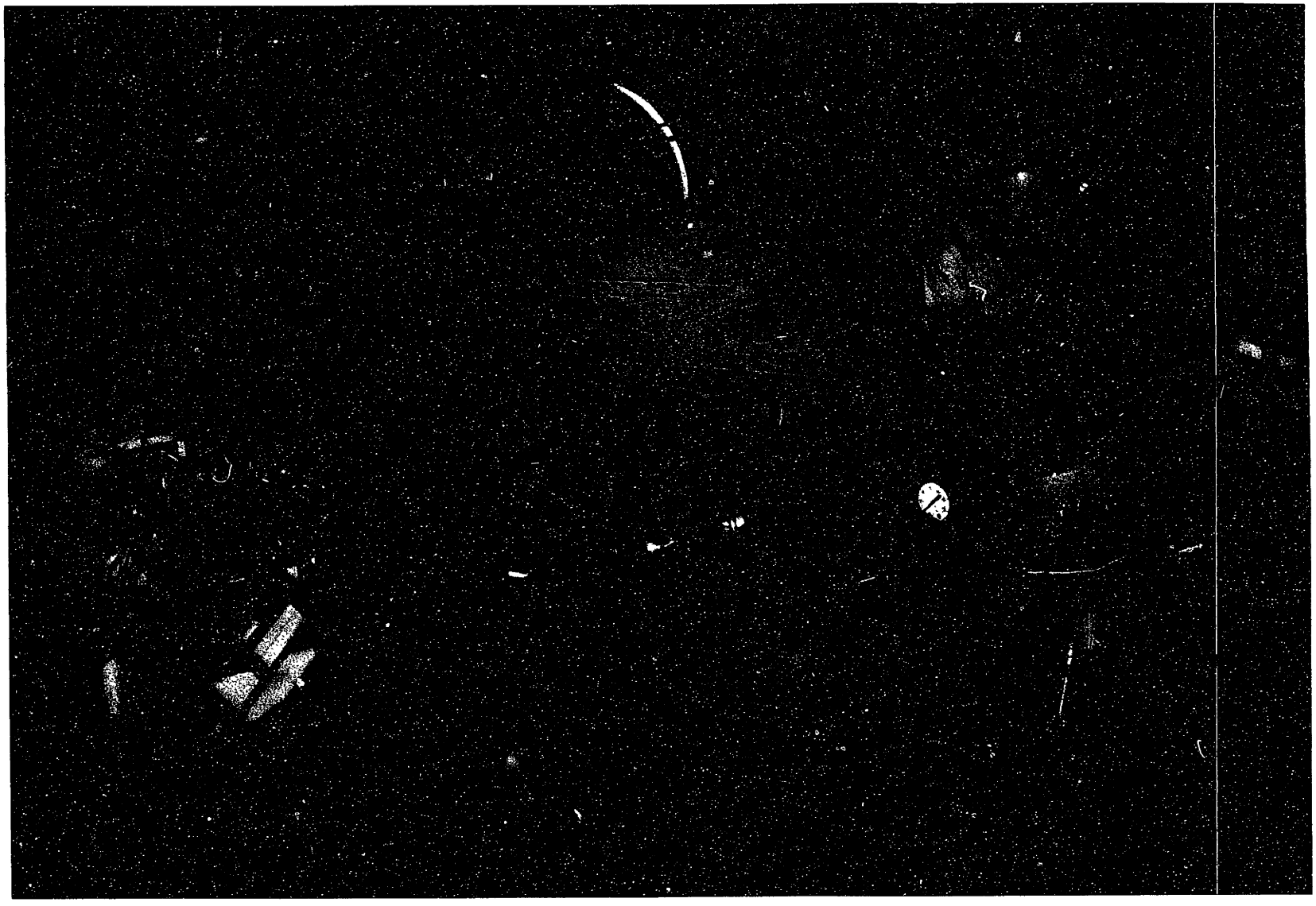

Fig 18 Turbo-alternator rig and associated instrumentation

air-turbine-design speed of 36,000 rpm. The following table summarizes some of the data taken at the various frequencies with balanced load resistances. Slip is defined as positive for generator action, that is, $\frac{\omega_n - \omega_1}{\omega_1}$. The complete alternator data is included in the Appendix.

Nominal Speed (rpm)	Stator Frequency (cps)	Slip (per unit)	Electrical Output Power (watts)	Capacitance/Phase (microfarads)
18,000	296	0.017	194	6.1
	295	0.020	240	6.1
	297	0.027	308	6.1
24,000	397	0.008	192	3.7
	396	0.010	260	3.7
	395	0.020	420	3.8
30,000	492	0.012	487	2.5
	498	0.014	536	2.4
	482	0.021	682	2.7
36,000	592	0.012	698	1.7
	592	0.013	832	1.8

The excitation current was in the range of 1.8 to 2.3 amperes which indicated that the degree of saturation was greater than the design value. As mentioned previously, this condition was expected for tests without external non-linearity in the excitation circuit. For the 600 cps run, 832 watts was the maximum output power that could be obtained because of turbine limitations. Maximum torque at 600 cps occurs at a slip of 0.085 so the induction machine operating at a slip of 0.013 was a substantial distance from its power limitations. The fact that the induction generator delivers 832 watts at 600 cps or 36,000 rpm and that power is proportional to speed assures at least 1400 watts at 1000 cps or 60,000 rpm.

During the tests it was observed that when the induction machine was allowed to coast down under load, it would not excite as readily on the next run as when the load was removed prior to the coast-down period. Load current flowing in the rotor bars during coast down tends to cancel the residual fluxes. The load and excitation voltages were observed on an oscilloscope and were sinusoidal for each frequency of operation.

Two interesting runs were made to test the inherent stability of the turbo-alternator combination. In the first run the alternator was loaded to 400 watts at 400 cps (24,000 rpm) and the capacity per phase was decreased in steps from 3.8 to 3.1 microfarads. The alternator did not lose excitation as might be expected from previous papers on induction generators but instead supplied increased power at successively higher speeds. Electrical output power increased from 420 watts at 3.8 microfarads to 460 watts at 3.1 microfarads, and speed increased from 24,200 rpm at 3.8 microfarads to 27,200 rpm at 3.1 microfarads. The speed increments varied in proportion to the changes in capacitance. The action of the induction machine was primarily due to the characteristics of the prime mover. With a decrease in excitation capacitance, the load and excitation voltages both decreased. This resulted in a decrease in electrical output power. A surplus of mechanical power was then available to accelerate the rotor until the power balance was restored. Had the prime mover been a constant speed machine such as a synchronous motor, the induction generator would have lost excitation as capacitance was decreased.

In the second run the induction generator was loaded to 400 watts at 500 cps (30,000 rpm), and both load resistances were decreased until rated current was reached in the load windings. Again the alternator did not lose excitation and delivered constant electrical power as the load resistances were decreased. Throughout the run, the capacitance per phase was maintained constant at 2.4 microfarads. The variation of load and excitation currents and voltages, stator frequency and rotational speed as a function of load resistance is shown graphically in Figure 19.

The curves in Figure 19 show that as load resistance is decreased, excitation current decreases linearly, load and excitation voltages decrease, load current increases and speed and stator frequency first decrease and then increase. The behavior can again be explained in terms of turbine characteristics. For a given setting of the input air valve, the turbine is essentially a constant-power device and turbine torque is inversely proportional to speed. With a constant input mechanical power, machine losses plus machine output power must equal a constant. The results in Figure 19 indicate that as load winding I^2R losses increased, excitation winding I^2R losses and core losses decreased.

With the assumption of constant losses, electrical power per phase is a constant.

$$I_L^2 R_L = k$$

If this expression is differentiated, the following results are obtained:

$$2I_L R_L dI_L + I_L^2 dR_L = 0$$

$$\frac{dI_L}{dR_L} = -\frac{I_L}{2R_L} \qquad (18)$$

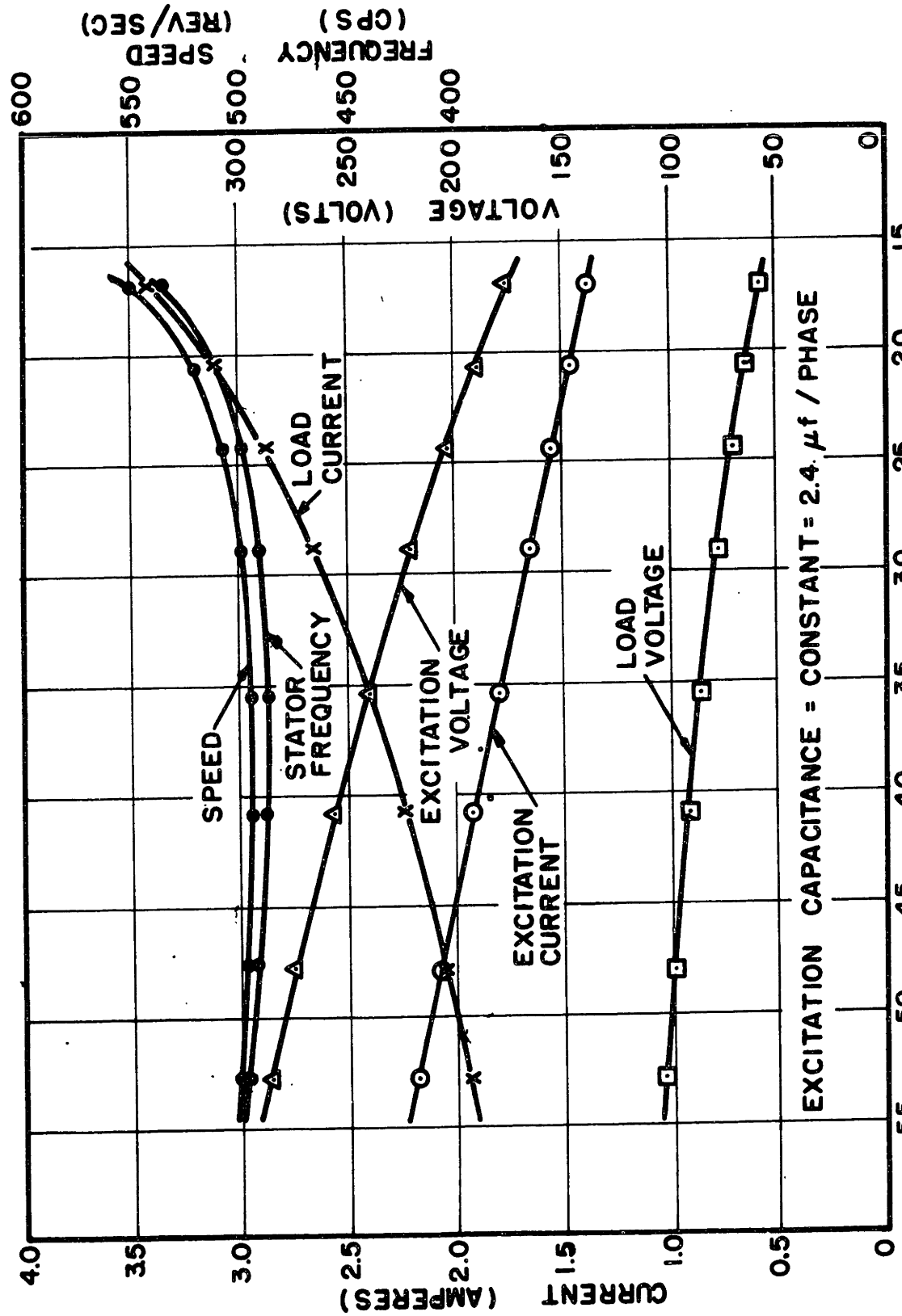

Fig. 19 Changes in load and excitation voltages and currents, stator frequency, and speed as generator load resistance is decreased.

When the load power per phase is expressed as $E_L I_L$ and the expression differentiated, equation (19) results.

$$\frac{dE_L}{dR_L} = -\frac{dI_L}{dR_L} R_L = \frac{I_L}{2} \tag{19}$$

The curves of load voltage and current in Figure 19 satisfy equations (18) and (19).

Since the turbine torque is inversely proportional to speed, the speed curve in Figure 19 indicates that the alternator counter torque must have first increased and then decreased. The curves also show that the slip increased as load resistance decreased. The reason for this can also be traced to the constant power characteristics of the prime mover.

For constant power $-\frac{1+s}{s} r_2 I_2^2 = k_1$ where s is defined as positive for generation action

assume $I_L = I_2$ (a good assumption for this particular machine because excitation current does not flow in the load windings)

$$\frac{1+s}{s} I_L^2 = k_2$$

Differentiating with respect to R_L yields

$$\frac{ds}{dR_L} = \frac{2s(s+1)}{I_L} \frac{dI_L}{dR_L}$$

If $\frac{dI_L}{dR_L}$ from equation (18) is substituted in this expression,

$$\frac{ds}{dR_L} = -\frac{s(s+1)}{R_L} \quad . \tag{20}$$

For small values of slip when (1+s) is approximately 1.0, equation (20) says that the fractional increase in slip is the same as the fractional decrease in load resistance for a constant-power prime mover.

The torque changes are more difficult to explain analytically. Torque in an induction machine is directly proportional to the product of the rotor resistance and the square of the rotor current and inversely proportional to the product of slip and stator frequency. For a 2-pole, 2-phase machine, the torque can be written as

$$T = -\frac{I_2^2 r_2}{\pi f s} = -\frac{I_L^2 r_2}{\pi f s} \qquad \text{if } I_2 = I_L . \tag{21}$$

The minus sign is introduced into the equation by the generator definition for s and shows that the torque is a counter torque in opposition to rotation. Since only generator operation is being considered in this discussion, the negative sign can be dropped. The variation of the product of torque and stator frequency with load resistance can be obtained if both sides of equation (21) are multiplied by f and the equation differentiated with respect to R_L.

$$\frac{d(Tf)}{dR_L} = \frac{r_2}{\pi}\left(\frac{2I_L}{s}\frac{dI_L}{dR_L} - \frac{I_L^2}{s^2}\frac{ds}{dR_L}\right)$$

If equations (18) and (20) are substituted for $\frac{dI_L}{dR_L}$ and $\frac{ds}{dR_L}$, respectively, and the result simplified, equation (22) is obtained.

$$\frac{d(Tf)}{dR_L} = \frac{r_2}{\pi}\left(\frac{I_L^2}{R_L}\right) = \frac{r_2}{\pi}\left(\frac{P_L}{R_L^2}\right) \tag{22}$$

This equation shows that for a constant-power prime mover the product of torque and stator frequency decreases if load resistance is decreased. For constant increments of R_L, the (Tf) increments vary inversely as R_L^2.

The value of stator frequency is determined by the reactive power balance in the machine and is also related to the speed through the slip. A careful study of the equivalent circuit and Figure 19 would show that the changes in currents and voltages in the machine with load resistance require frequency to first decrease and then increase to maintain the reactive power balance. Once frequency is determined, speed and torque are set by the torque-speed curve of the turbine and the slip. Indications of torque and slip changes with load resistance can be obtained from equations (20) and (22), but a complete solution would require a more detailed analysis such as Mr. Peake is working on.

IX

CONCLUSIONS

The results and analyses of the motor and alternator tests as presented in Sections VII and VIII indicate that the induction machine that was designed meets the alternator and motor requirements outlined in the Introduction. The machine does not have the minimum possible volume because test life rather than operating life was used to set the flux and current densities. Tests also show that a turbine and capacitor-excited-induction-generator combination exhibits more inherent stability than a capacitor-excited induction generator coupled to a constant speed drive. The stable performance can be primarily attributed to the constant-power characteristic of the drive turbine.

After completing the detailed designing process, the author feels that there is substantial room for improvement in classical techniques, particularly in the design of high frequency machines. The approach outlined in Section II where densities and dimensions are initially chosen from volt-ampere and speed requirements is a gain over the technique of initially designing for voltage or current separately. The trial and error technique of making the voltage design compatible with the current design is eliminated, and the initial dimensions are nearly the same as the final dimensions.

The use of normalized reactance formulas gives far more insight into machine performance and shows at a glance how a design change is

going to affect reactance. For example, with a given volt-ampere requirement, changes in number of turns alone will have no affect on the per-unit reactance and hence, on the machine performance. However, the appearance of N^2 in the classical equations for ohmic reactance may lead to the erroneous conclusion that machine performance can be improved by decreasing the number of turns.

The normalizing process can be extended to include the formulas for stator and rotor resistances and thus allow a complete per-unit equivalent circuit in terms of design quantities. With such a circuit machine synthesis is possible and machine design can attain the same high level as machine analysis.

APPENDIX

1. Derivation of Equation (1)

The standard equation for the induced voltage in the stator windings of an a-c machine is

$$E = 4.44 f N k_w \varphi_p \times 10^{-8}$$

N = series turns/phase

φ_p = flux/pole in lines

f = frequency in cps

E = volts/phase

k_w = winding factor

If the maximum flux in the air gap is defined as φ_t as in Kuhlmann's book and a sinusoidal air-gap flux distribution is assumed,

$$\varphi_p = \frac{2}{\pi} \varphi_t \left(\frac{1}{p}\right)$$ p = number of poles

$$B_g = \frac{\varphi_t}{\pi DL}$$ B_g = maximum flux density in air gap in lines/in^2

or $\varphi_t = \pi DLB_g$

If this is substituted in the above relation containing φ_p and φ_t, the following expression for φ_p is obtained:

$$\varphi_p = \frac{2}{p} DLB_g$$

and $$E = \frac{8.88}{p} N f k_w DLB_g \times 10^{-8}$$

since $\frac{f}{p} = \frac{n}{120}$ where n = synchronous speed in rpm

$$E = 0.074 N k_w DLB_g n \times 10^{-8}$$

The current per phase, I, equals the product of conductor area and current density.

$$I = \frac{S_c A}{2Nm}$$

S_c = total stator conductor cross-sectional area in inch^2

A = current density in amperes/in^2

m = number of phases

The total volt amperes of the machine equal the product of phase voltage, phase current and number of phases.

$$(VA) = EIm$$

$$= (0.074Nk_w DLB_g n \times 10^{-8}) \left(\frac{S_c A}{2Nm}\right) m$$

$$= 0.037 k_w DLB_g n S_c A \times 10^{-8}$$

or

$$k_w AB_g DLS_c = \frac{27 \times 10^8 (VA)}{n} \qquad \text{Equation (1)}$$

2. Derivation of Equations (2), (3) and (4)

The I^2R losses in a conductor can be expressed as follows:

$$P = (Aa)^2 \left(\frac{\rho \ell}{a}\right)$$

$$= A^2 \rho (a \ell)$$

$$= A^2 \rho V$$

P = power in watts

A = current density in amperes/in^2

ℓ = conductor length in inches

a = conductor area in inches^2

V = conductor volume in inches^3

ρ = resistivity = ohms/inch cube

If heat dissipation is neglected, the following equation for stored energy can be written:

$Pt = C\theta W$

t = time in seconds

C = thermal capacity in $\frac{\text{joules}}{\text{lb.}}$/degrees C.

θ = temperature rise in degrees Centigrade

W = weight in lb.

The expression for P in terms of A, ρ and V can be substituted in the energy equation to obtain

$$A^2 \rho V t = C\theta W$$

$$A = \sqrt{\frac{W}{V} \frac{C\theta}{\rho t}} \qquad d = \text{density in } \frac{\text{lb.}}{\text{in}^3}$$

$$= \sqrt{d \frac{C\theta}{\rho t}}$$

The following values for ρ, C and d for copper and aluminum are from the book, "Electromagnetic Devices", by H. C. Roters.

	ρ(ohms/inch cube at 75°C.)	C($\frac{\text{joules}}{\text{lb.}}$/degrees C.)	d(lb/in^3)
copper	0.83×10^{-6}	180	0.32
aluminum	1.36×10^{-6}	433	0.093
steel		225	0.28

If these values are substituted in the above equation for A, the following equations are obtained:

copper $\quad A = \sqrt{1.15 \times 10^6 \frac{\theta}{t}}$ $\quad$ Equation (2)

aluminum $\quad A = \sqrt{0.49 \times 10^6 \frac{\theta}{t}}$ $\quad$ Equation (3)

where t now represents time in minutes.

In the case of core loss, the logical quantity to use in a study of temperature rise is watts/pound which can be readily determined for a

specified lamination thickness, flux density and frequency from published data. If heat dissipation is neglected as before

$$pt = C\theta \qquad \text{where } p = \text{watts/pound}$$

With t in minutes and the value of C for steel

$$p = 3.75\,\frac{\theta}{t} \qquad \text{Equation (4)}$$

3. Derivation of Equations (7), (8), (9) and (10)

The first step in a derivation of normalized equations for reactances must be the development of an expression for base ohms.

$$\text{base ohms} = \frac{E}{I} = \frac{E}{(VA)/mE} = \frac{mE^2}{(VA)}$$

In the derivation of Equation (1), E was expressed as

$$E = \frac{8.88}{p}\,Nfk_w DLB_g \times 10^{-8}$$

$$\text{base ohms} = \frac{m}{(VA)}\left(\frac{8.88}{p}\,Nfk_w DLB_g \times 10^{-8}\right)^2 = \frac{78.8 \times 10^{-16}(k_w f B_g DLN)^2 m}{p^2(VA)}$$

The following design formulas for ohmic values of principle leakage and magnetizing reactances were taken from the "Induction Motor Design Notes" of R. B. Bross of the Instrumentation Laboratory. The only change made in the equations was to substitute series turns/phase for series conductors/phase.

$$X_s = \frac{80f(Nk_w)^2 L m K_s \times 10^{-8}}{S_s} = \text{slot leakage reactance}$$

$$X_{zz} = \frac{26.7f(Nk_w)^2 LmK_{zz} \times 10^{-8}}{S_s \delta} = \text{zig-zag leakage reactance}$$

$$X_e = \frac{39.4f(Nk_w)^2 m(D + d_s)(CT) \times 10^{-8}}{S_s p} = \text{end turn leakage reactance}$$

$$X_M = \frac{25.6f(Nk_w)^2 mLD \times 10^{-8}}{\delta k_s k_r k_{sat} p^2} = \text{magnetizing reactance}$$

The symbols are defined on Page 13.

The normalized or per unit reactances are obtained by dividing each of the equations for ohmic values of reactance by the base ohms. When this is done, the following equations are obtained:

$$\text{per unit } X_s = \frac{1.02p^2(VA)K_s \times 10^8}{fB_g^2 D^2 L S_s} \qquad \text{Equation (7)}$$

$$\text{per unit } X_{zz} = \frac{0.339p^2(VA)K_{zz} \times 10^8}{fB_g^2 D^2 L \delta S_s} \qquad \text{Equation (8)}$$

$$\text{per unit } X_e = \frac{0.500(1 + d_s/D)p(CT) \times 10^8}{fB_g^2 D L^2 S_s} \qquad \text{Equation (9)}$$

$$\text{per unit } X_M = \frac{0.325(VA) \times 10^8}{k_s k_r k_{sat} f B_g^2 D L \delta} \qquad \text{Equation (10)}$$

4. Calculations for Figure 3

The following equation for the effective resistance of the embedded part of the stator winding in one slot was obtained from Chapter 7 of "Electrical Coils and Conductors" by H. B. Dwight.

For copper at 75° Centigrade

$$\frac{R_{AC}-R_{DC}}{R_{DC}} = \left(\frac{h^2 fW}{8.23S}\right)^2 \left(\frac{4}{9}(q')^2 - \frac{1}{45} - \frac{1}{3}(q')^2 \sin^2 \frac{\varphi}{2}\right)$$

(terms of higher order in Bessel series neglected)

where h = height of one wire measured perpendicular to direction of leakage flux = bare wire diameter in inches for round wire

f = frequency in cps

W = net amount of copper measured horizontally across the slot

s = width of slot

q' = the number of rows of conductors one above the other in the <u>half slot</u>

φ = phase angle between currents in upper and lower coil side

Neglect $\frac{1}{45}$ as compared with the other terms in the parentheses and let "q" equal the number of rows of conductors one above the other in the <u>entire slot</u> and b equal $\frac{W}{s}$, the per-unit width of conducting material in the slot.

Then $$\frac{R_{AC}-R_{DC}}{R_{DC}} = \left(\frac{h^2 fbq}{16.5}\right)^2 \left(\frac{4}{9} - \frac{1}{3} \sin^2 \frac{\varphi}{2}\right)$$

If "a" equals the fraction of slots with windings out of phase, $\frac{R_{AC}-R_{DC}}{R_{DC}}$ for all of the embedded part of the stator winding equals

$$\left(\frac{h^2 fbq}{16.5}\right)^2 \left[\frac{4}{9}(1-a) + a\left(\frac{4}{9} - \frac{1}{3} \sin^2 \frac{\varphi}{2}\right)\right] = \left(\frac{h^2 fbq}{16.5}\right)^2 \left[\frac{4}{9} - \frac{a}{3} \sin^2 \frac{\varphi}{2}\right]$$

For 2-phase windings, φ equals 90° and for 3-phase windings, φ equals 60°.

For 2-phase windings

$$\frac{R_{AC}-R_{DC}}{R_{DC}} = \left(\frac{h^2 fbq}{16.5}\right)^2 \left[\frac{4}{9}-\frac{a}{6}\right]$$

For 3-phase windings

$$\frac{R_{AC}-R_{DC}}{R_{DC}} = \left(\frac{h^2 fbq}{16.5}\right)^2 \left[\frac{4}{9}-\frac{a}{12}\right]$$

If the second term in each of the expressions in parentheses were neglected, the maximum error would result when all the coil sides in the tops and bottoms of slots were out of phase. This error would equal 17% for a 2-phase winding and 8% for a 3-phase winding. In general, all of the slots will not contain out-of-phase coil sides. As an approximation, "a" is taken equal to zero.

$$\frac{R_{AC}-R_{DC}}{R_{DC}} = \left(\frac{h^2\,\alpha}{24.7}\right)^2 \qquad \text{where } \alpha = fbq$$

This equation is plotted in Figure 3 for values of "h" corresponding to the bare wire diameter of wire sizes 14 to 30.

Because the equation only holds for the embedded part of the stator winding, the effective resistance of the entire winding is less than the value given by the curves of Figure 3. If β equals $\frac{R_{AC}-R_{DC}}{R_{DC}}$ for the embedded part and "c" equals the ratio of armature core length to mean conductor length, $\frac{R_{AC}-R_{DC}}{R_{DC}}$ for the entire winding equals $c\beta$ or $R_{AC} = (1+c\beta)R_{DC}$.

5. Calculations for Figure 4

The zig-zag permeance factor K_{zz} is defined in P. L. Alger's book, "The Nature of Polyphase Induction Machines", and R. B. Bross's "Induction Motor Design Notes" as follows:

$$K_{zz} = \frac{\left[(b_s - a_s) + (b_r - a_r)\right]^2}{4(b_s + b_r)}$$

where a_s = the stator slot opening at the air gap

a_r = the rotor slot opening at the air gap

b_s = the stator slot pitch at the air gap

b_r = the rotor slot pitch at the air gap

If the b's and a's in the numerator are grouped together and the expression divided by δ

$$\frac{K_{zz}}{\delta} = \frac{\left[(b_s + b_r) - (a_s + a_r)\right]^2}{4(b_s + b_r)\delta}$$

Let $\bar{a} = \frac{a_s + a_r}{2}$ = average slot opening at the air gap

and $\bar{b} = \frac{b_s + b_r}{2}$ = average slot pitch at the air gap

$$\frac{K_{zz}}{\delta} = \frac{(2\bar{b} - 2\bar{a})^2}{4(2\bar{b})\delta} = \frac{\left(\frac{\bar{b}}{\bar{a}} - 1\right)^2 \bar{a}^2}{2\bar{b}\delta} = \frac{\left(\frac{1}{\bar{a}/\bar{b}} - 1\right)^2 \frac{\bar{a}}{\bar{b}}}{2\delta/\bar{a}}$$

This expression for $\frac{K_{zz}}{\delta}$ is plotted in Figure 4 for various ratios of gap length to slot opening and slot opening to slot pitch.

6. Detail of the Windings of the 60,000 rpm machine

The winding layout of the 60,000 rpm machine is shown in Figure 20. Only the end connections are shown in the figure, and the line for each phase represents both the 400 and 150 volt windings.

For balanced leakage reactances in the two-phase windings, the same number of coil sides of each phase should be in the bottoms of the slots. If form-wound coils are used, this condition is automatically satisfied

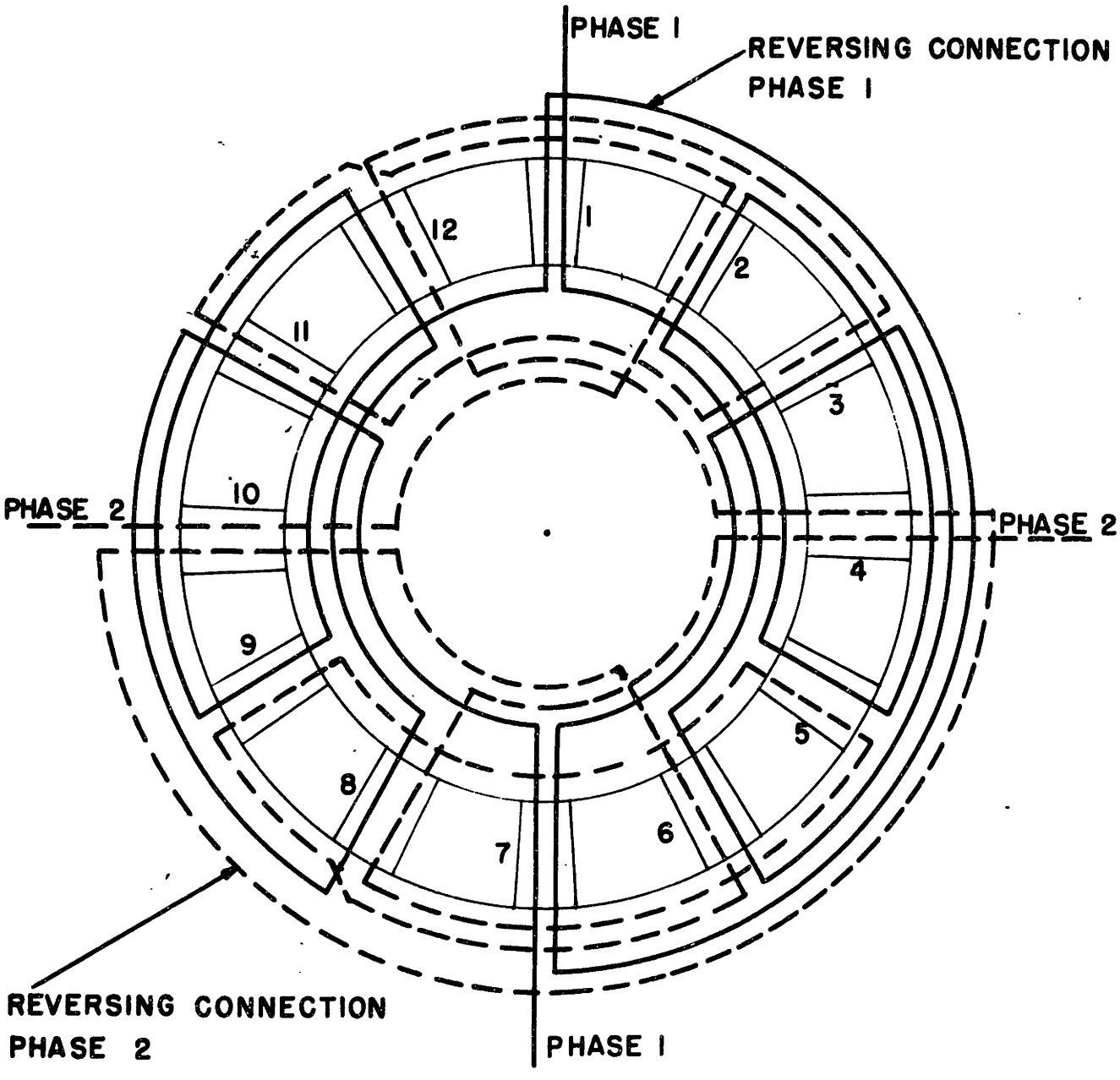

Fig.20 Winding layout of the 60,000 RPM induction machine

because all the bottom coil sides are placed in the slots first. In this machine there was insufficient area at the inside of the stator stack to accommodate half of the coil sides simultaneously, and random winding had to be employed. A cylindrical wooden form that had the same inside diameter as the aluminum yoke was clamped to both ends of the stator stack to serve as a guide during the winding process. Half of the windings for one phase was completed at a time as outlined in the following instructions. End "A" in the instructions refers to the end of the stator stack farther away from the mounting flange.

Winding Instructions for Random Winding of Stator

1. Insert .010" teflon liner in each slot.
2. Start in slot 1 with No. 24 wire at end A and tag wire.
3. Wind 42 turns around slots 1 and 5.
4. After completion of 42nd turn in slot 5 enter slot 2 on end A.
5. Wind 42 turns around slots 2 and 6.
6. After completion of 42nd turn in slot 6 enter slot 3 on end A.
7. Wind 42 turns around slots 3 and 7.
8. After completion of 42nd turn in slot 7 bring lead out on end A and allow more wire than was used in steps 2 to 7. Then cut wire.
9. Repeat steps 2-8 with No. 21 wire substituting "16" for "42" in all cases where "42" occurs. Tag wire entering slot 1.
10. Insert .010" teflon spacers in slots 1, 2, 3, 5, 6, and 7.
11. Start in slot 4 with No. 24 wire at end A and tag wire.
12. Wind 42 turns around slots 4 and 8.
13. After completion of 42nd turn in slot 8 enter slot 5 on end A.

14. Wind 42 turns around slots 5 and 9.
15. After completion of 42nd turn in slot 9 enter slot 6 on end A.
16. Wind 42 turns around slots 6 and 10.
17. After completion of 42nd turn in slot 10 bring lead out on end A. and allow more wire than was used in steps 11-16.
18. Repeat steps 11 to 17 with No. 21 wire substituting "16" for "42" in all cases where "42" occurs. Tag wire entering slot 4.
19. Insert .010" teflon spacers in slots 4, 8, 9, and 10.
20. Insert .030" teflon wedges in slots 5 and 6.
21. Pick up No. 24 wire leaving slot 10 and enter slot 4 on end A.
22. Wind 42 turns from slots 4 to 12.
23. After completion of 42nd turn in slot 12 enter slot 3 on end A.
24. Wind 42 turns from slots 3 to 11.
25. After completion of 42nd turn in slot 11 enter slot 2 on end A.
26. Wind 42 turns from slots 2 to 10.
27. After completion of 42nd turn in slot 10 bring lead out from stator on end A and tag wire.
28. Repeat steps 21 through 27 with No. 21 wire substituting "16" for "42" in all cases where "42" occurs. Tag wire leaving slot 10.
29. Insert .010" teflon spacers in slots 11 and 12.
30. Insert .030" teflon wedges in slots 2, 3, 4, and 10.
31. Pick up No. 24 wire leaving slot 7 and enter slot 1 on end A.
32. Wind 42 turns from slots 1 to 9.
33. After completion of 42nd turn in slot 9 enter slot 12 on end A.
34. Wind 42 turns from slots 12 to 8.

35. After completion of 42nd turn in slot 8 enter slot 11 on end A.

36. Wind 42 turns from slots 11 to 7.

37. After completion of 42nd turn in slot 7 bring lead out of stator on end A and tag wire.

38. Pick up No. 21 wire from slot 7 and complete steps 31-37 substituting "16" for "42" in all cases when "42" occurs. Tag wire leaving slot 7.

39. Insert .030" teflon wedges in slots 1, 7, 8, 9, 11, and 12.

40. Bundle tagged leads from slots 1, 4, 7, and 10 altogether and bring out through one axial hole in end bell near end A.

7. Calculation of Equivalent Circuit Constants

The resistances and reactances were calculated from formulas appearing in R. B. Bross's "Design Notes" and in Kuhlmann's book, "The Design of Electrical Apparatus".

(a) Stator resistance - 150 volt winding

$$r_{1L} = 2N_L \frac{(L_{MC})}{12} \frac{(\text{D-C resistance at } 25^{\circ}\text{C/1000FT})(\text{temperature factor})}{1000}$$

where N_L = series turns/phase = 96 for load winding

L_{MC} = length of mean conductor

$$L_{MC} = L + \frac{Y\left[(CT)\pi(D + d_s)\right]}{S_s}$$

L = core length = 1.5 inches

Y = end turn extension factor = 1.4 for a two-pole machine

CT = coil throw = 4 slots

D = air gap diameter = 1.5 inches

d_s = stator slot depth = 0.530 inches

S_s = stator slots = 12

$$L_{MC} = 1.50 + \frac{1.4\,[4\pi(2.03)]}{12} = 4.48 \text{ inches}$$

$$\frac{\text{D-C RES. at } 25^{\circ}\text{C}}{1000 \text{ FT}} = 13.0 \text{ ohms (for No. 21 wire)}$$

temperature factor = 1.21 for 75° Centigrade

With these values $r_{1L} = 1.13$ ohms

(b) Stator resistance - 400 volt winding

The equation is the same as that used above to calculate r_{1L}. However, for the 400 volt winding, N_L becomes N_x and the d-c resistance is different.

$N_x = 252$ series turns/phase

$$\frac{\text{D-C RES. at } 25^{\circ}\text{C}}{1000 \text{ FT}} = 26.2 \text{ ohms (for No. 24 wire)}$$

With these changes and the values listed above $r_{1x} = 5.96$ ohms

(c) Rotor resistance referred to load winding

$$r_2 = 4(N_L k_w)^2 m\rho(B+R) \text{ ohms}$$

N_L is the same as in the calculation of r_{1L}

k_w = winding factor = 0.790

m = phases = 2

ρ = resistivity = 0.83×10^{-6} ohms/inch cube at 75°C (copper)

$$B = \frac{\text{LENGTH}}{\text{AREA}} \text{ for bars} = \frac{\sqrt{L_R^2 + (Sk)^2}}{S_r a_b}$$

L_R = rotor stack length = 1.56 inches

Sk = skew = 0.393 inches

S_r = rotor slots = 17

a_b = area of one bar = 0.0206 inches^2 (No. 6 wire)

$$B = \frac{\sqrt{1.56^2 + 0.393^2}}{17 \times 0.0206} = 4.60$$

$$R = \frac{\text{LENGTH}}{\text{AREA}} \text{ for end ring} = \frac{2}{\pi} \frac{D_{ring}}{a_r p^2} K_{ring}$$

D_{ring} = mean diameter of end ring

D_{ring} = (rotor diameter) - (slot depth) = $1.440 - 0.193 = 1.247$ in.

a_r = area of end ring

a_r = (axial length) x (radial length) = $0.25 \times 0.20 = 0.05$ in^2

p = poles = 2

K_{ring} = end-ring current distribution constant from P. H. Trickey's paper, "Induction Motor Resistance Ring Width"

$K_{ring} = 0.93$

$$R = \frac{2}{\pi} \frac{1.247}{0.05 \times 2^2} 0.93 = 3.69$$

With these values $r_2 = 0.319$ ohms

(d) Leakage and magnetizing inductances

Before ℓ_{1L}, ℓ_{1x}, ℓ'_1, and ℓ_2 could be calculated, the stator and rotor slot leakage inductances, zig-zag inductance, end-turn inductance, skew leakage inductance, and belt leakage inductance had to be computed. An equation for each of these was obtained by dividing the corresponding reactance formula in R. B. Bross's notes or Kuhlmann's book by $2\pi f$.

ℓ_{ss_L} = stator slot leakage inductance referred to load winding

$$\ell_{ss_L} = \frac{12.7(Nk_w)^2 LmK_{ss} \times 10^{-8}}{S_s} \text{ henries}$$

N = series turns/phase = 96

k_w = winding factor = 0.912 x 0.866 = 0.790

L = average stack length = 1.53 inches

m = phases = 2

S_s = stator slots = 12

K_{ss} = stator slot factor = $C_x F_{ss}$

C_x = pitch correction factor = 1.07

F_{ss} = relative slot permeance = 0.842 for slot dimensions in Figure 8 (see Kuhlmann, p. 356)

With these values ℓ_{ss_L} = 0.168 millihenries

ℓ_{sr_L} = rotor slot leakage induction referred to load winding

$$\ell_{sr_L} = \frac{12.7(Nk_w)^2 LmK_{sr} \times 10^{-8}}{S_r} \text{ henries}$$

L, N, k_w and m are the same as in the calculation of ℓ_{ss_L}.

S_r = rotor slots = 17

K_{sr} = relative slot permeance

K_{sr} = 1.223 for dimensions in Figure 8 (Kuhlmann, p. 356)

With these values ℓ_{sr_L} = 0.161 millihenries

ℓ_{zz_L} = zig-zag leakage inductance referred to load winding

$$\ell_{zz_L} = \frac{4.25(Nk_w)^2 LmK_{zz} \times 10^{-8}}{S_s \delta} \text{ henries}$$

N, k_w, L, m and S_s are the same as in the calculation of ℓ_{ss_L}.

K_{zz} = air-gap geometry factor

$$K_{zz} = \frac{\left[(b_s - a_s) + (b_r - a_r)\right]^2}{4(b_s + b_r)}$$

where a_s, b_s, a_r, and b_r are defined in Figure 4

$$b_s = \frac{\pi D_s}{S_s} = 0.393 \text{ inches}$$

$$b_r = \frac{\pi D_r}{S_r} = 0.266 \text{ inches}$$

a_s = 0.100 inches (from Figure 8)

a_r = 0.050 inches (from Figure 8)

$$K_{zz} = \frac{\left[(0.393 - 0.100) + (0.266 - 0.050)\right]^2}{4(0.393 + 0.266)} = 0.0983$$

δ = air-gap length = 0.030 inches

With these values ℓ_{zz_L} = 0.204 millihenries

ℓ_{e_L} = end-turn leakage inductance referred to load winding

$$\ell_{e_L} = \frac{6.28(Nk_w)^2 m(D + d_s)(CT) \times 10^{-8}}{S_s p} \text{ henries}$$

N, k_w, m and S_s are the same as in the calculation of ℓ_{ss_L}

D = air-gap diameter = 1.50 inches

d_s = stator slot depth = 0.53 inches

(CT) = coil throw = 4 slots

p = poles = 2

With these values ℓ_{e_L} = 0.244 millihenries

ℓ_m = magnetizing inductance referred to the load winding

$$\ell_m = \frac{4.07(Nk_w)^2 mLDC_{sk} \times 10^{-8}}{\delta k_s k_r k_{sat} p^2} \text{ henries}$$

where N, k_w, m, L, D, δ and p are the same as in the above leakage inductance calculations.

$$k_{sat} = 1 + \frac{(AT)_{iron}}{(AT)_{gap}} = 1.08$$ for flux corresponding to rated voltage and frequency

(See Flux Density and Core Loss Table in Section V)

$$k_s = \frac{1}{1 - \frac{a_s^2}{b_s(5\delta + a_s)}} = \frac{1}{1 - \frac{(0.100)^2}{0.393(5 \times 0.030 + 0.100)}} = 1.115$$

$$k_r = \frac{1}{1 - \frac{a_r^2}{b_r(5\delta + a_r)}} = \frac{1}{1 - \frac{(0.050)^2}{0.293(5 \times 0.030 + 0.050)}} = 1.06$$

C_{sk} = skew correction factor (approx. 1.0) = $\dfrac{\sin \frac{\theta_{sk}}{2}}{\frac{\pi\theta_{sk}}{360}}$

θ_{sk} = angle of skew in degrees

$$\theta_{sk} = \frac{SKEW \times 180}{\frac{\pi D}{p}} = \frac{0.393 \times 180}{\pi \times \frac{1.5}{2}} = 30^\circ$$

$$C_{sk} = \frac{\sin 15^\circ}{\frac{\pi}{360} \times 30} = 0.989$$

With these values ℓ_m = 6.97 millihenries

ℓ_m referred to excitation winding = $\left(\frac{N_x}{N_L}\right)^2$ 6.97 = 48.1 millihenries

ℓ_{sk_L} = skew leakage reactance referred to load winding

$$\ell_{sk_L} = \ell_m \left(\frac{\theta_s}{199}\right)^2 K_p$$

where
$$K_p = \sqrt{\frac{\ell_m}{\left[1+\left(\frac{\theta_s}{199}\right)^2\right]\ell_m + \ell_{s_L} + \ell_{zz_L} + \ell_{e_L}}}$$

θ_s = angle of skew defined above = 30°

ℓ_m = magnetizing inductance referred to load winding = 6.97 millihenries

ℓ_{s_L} = total slot leakage inductance referred to load winding = 0.329 millihenries

ℓ_{zz_L} = zig-zag leakage inductance referred to load winding = 0.204 millihenries

ℓ_{e_L} = end turn leakage inductance referred to load winding = 0.244 millihenries

$$K_p = \sqrt{\frac{6.97}{\left[1+\left(\frac{30}{199}\right)^2\right]6.97 + 0.329 + 0.204 + 0.244}} = 0.938$$

With these values ℓ_{sk_L} = 0.148 millihenries

ℓ_{B_L} = Belt leakage reactance referred to load winding

$$\ell_{B_L} = 0.00364\, \ell_m \frac{K_B}{C_{sk}}$$

where K_B = belt factor (depends upon number of stator and rotor slots and number of poles)

K_B from plot No. 69 in R. B. Bross's "Design Notes" = 1.98

ℓ_m = 6.97 millihenries

C_{sk} = 0.989

With these values ℓ_{B_L} = 0.051 millihenries

ℓ_{1L}, ℓ_{1x}, ℓ'_1, and ℓ_2 can now be computed.

$$\ell_{1L} = \ell_{ss_L} + \frac{\ell_{e_L}}{2} = 0.168 + \frac{0.244}{2} = 0.290 \text{ millihenries}$$

$$\ell'_1 = \frac{1}{2}(\ell_{zz_L} + \ell_{sk_L} + \ell_{B_L}) = \frac{1}{2}(0.204 + 0.148 + 0.051) = 0.202 \text{ millihenries}$$

$$\ell_2 = \frac{1}{2}(\ell_{zz_L} + \ell_{sk_L} + \ell_{B_L} + \ell_{e_L}) + \ell_{sr} = \frac{1}{2}(0.204 + 0.148 + 0.051 + 0.244) + 0.161$$

ℓ_2 = 0.484 millihenries

The excitation winding sees the same magnetic circuit as the load winding so ℓ_{1x} can be computed from ℓ_{1L}.

$$\ell_{1x} = \left(\frac{N_x}{N_L}\right)^2 \ell_{1L} = \left(\frac{252}{96}\right)^2 0.290 = 2.00 \text{ millihenries}$$

8. Data from Conventional Induction-Motor Tests

Note: Phase 1 refers to winding entering slot 1 and leaving slot 7 and phase 2 refers to winding entering slot 4 and leaving slot 10.

Blocked-Rotor Tests at 60 cps (2-Phase Voltages Applied)

	400-Volt Winding (150-Volt Winding Open-Circuited)		150-Volt Winding (400-Volt Winding Open-Circuited)	
	Phase 1	Phase 2	Phase 1	Phase 2
Voltage (volts)	7.3	7.3	3.2	3.3
Current (amperes)	0.98	0.95	2.41	2.35
Power (watts)	6.75	6.6	7.5	7.5

No-Load Tests at 60 cps (2-Phase Voltages Applied)

	400-Volt Winding (150-Volt Winding Open-Circuited)		No-Load Test at Reduced Voltage for Friction and Windage 400-Volt Winding	
	Phase 1	Phase 2	Phase 1	Phase 2
Voltage (volts)	22	22	12	12
Current (amperes)	1.03	1.02	0.4	0.5
Power (watts)	7.2	6.7	2.2	2.2

Approximate No-Load Speed 3600 rpm

Blocked-Rotor Tests at 400 cps (2-Phase Voltages Applied)

	400-Volt Winding (150-Volt Winding Open-Circuited)		150-Volt Winding (400-Volt Winding Open-Circuited)	
	Phase 1	Phase 2	Phase 1	Phase 2
Voltage (volts)	22.3	22.3	6.9	7.1
Current (amperes)	1.01	1.01	2.5	2.5
Power (watts)	9.5	8.5	9.7	10

No-Load Tests at 400 cps (2-Phase Voltages Applied)

	400-Volt Winding (150-Volt Winding Open-Circuited)		No-Load Test at Reduced Voltage for Friction and Windage 400-Volt Winding	
	Phase 1	Phase 2	Phase 1	Phase 2
Voltage (volts)	75	73	25	24.3
Current (amperes)	0.60	0.52	0.40	0.43
Power (watts)	5.0	18.0	7.5	8.5

Approximate No-Load Speed 24,000 rpm

9. Data from Motor Load Tests

Notes: 1. Circuit diagram is shown in Figure 13.

2. All motor tests were made with 400-volt windings excited from 2-phase Scott connection and 150-volt windings open-circuited.

3. Dynamometer torque readings include friction and windage.

4. Torque arm of dynamometer equals 11 inches.

5. Run 1 - duration 20 minutes

   (a) Motor was brought up to speed with 100 cps voltages applied.

   (b) Source frequency was then increased gradually to 400 cps.

6. Run 2 - duration 35 minutes

   (a) Motor was brought up to speed with 200 cps voltages applied.

   (b) Readings past the third set were obtained by decreasing applied voltage.

7. Run 3 - duration 20 minutes

   (a) Motor was brought up to speed with 300 cps voltages applied.

   (b) Torque readings are not reliable because dynamometer housing was not properly zeroed prior to run.

8. Run 4 - duration 20 minutes

   (a) Motor was brought up to speed with 65 volts/phase 400 cps applied.

   (b) Dynamometer was zeroed properly.

9. Results of runs 2 and 4 are plotted in Figures 14 and 15, respectively, with data corrected to 50 volts and 115 volts. In Figures 14 and 15, friction and windage torques estimated from the reduced voltage no-load tests were added to the measured readings.

			Phase 1			Phase 2			
	Input Freq. (cps)	Shaft Speed (Rev/Sec)	Voltage (Volts)	Current (Amps)	Power (Watts)	Voltage (Volts)	Current (Amps)	Power (Watts)	Torque (Oz)
Run 1	398	383	81.5	1.45	95	81.5	1.42	93	1.0
	398	375	82	1.77	112	82	1.70	110	1.0+
	398	366	80	2.07	133	80	2.02	130	1 3/16
	398	350	60	1.90	84	60	1.90	82	1.0+
Run 2	206	201	46	0.80	21	46	0.81	21.6	3/8
	206	197	45.5	1.00	35	45.5	1.00	35.4	9/16
	206	191	44.2	1.30	48	44.7	1.31	50	3/4
	205	189	44	1.39	53.2	44.2	1.42	54	13/16
	206	165	41.7	2.10	75	42.7	2.17	79	7/8
	205	157	41	2.18	75.4	41	2.19	76	7/8
	205	152	39.5	2.18	73	39.5	2.14	72	3/4
	205	139	38	2.26	70	38	2.24	70	5/8
	205	132	37	2.26	69	37	2.25	68	1/2
	205	75	30	2.28	47	30	2.26	47	1/4
Run 3	293	282	57	0.90	37	57	0.90	37	7/8
	291	267	54	1.57	68.4	54	1.54	68	1 5/8
	291	240	52	2.23	89.4	52	2.19	88	1 5/8
	292	227	50.8	2.37	88	51	2.32	88	1 1/2
	292	195	48	2.46	83	48	2.39	80	1 1/4
Run 4	400	394	115	1.05	65	115	1.01	65	3/4
	400	389	113	1.52	129	113	1.52	130	1 5/16
	400	386	112	1.69	146.4	112	1.67	148	1 1/2
	400	383	111	1.84	162	112	1.86	164	1 9/16
	400	379	110	2.14	190	110.5	2.14	193	1 5/8
	400	376	109	2.19	194	110	2.22	198	1 3/4
	400	364	99	2.62	204	99.5	2.56	204	1 5/8

10. Calculation of Torque-Speed Points from Design Quantities

The method of calculation employed below is based on the procedure developed by C. G. Veinott in his paper "Performance Calculations of Induction Motors". Certain "F" constants which depend on the equivalent circuit constants of the machine are first evaluated, and then torque calculations can be rapidly made for various values of slip.

ℓ_{BR} = blocked rotor inductance of 400 volt winding

$$= \ell_{1x} + \left(\frac{N_x}{N_L}\right)^2 (\ell_1' + \ell_2) = 2.00 + \left(\frac{252}{96}\right)^2 (0.202 + 0.484) = 6.73 \text{ millihenries}$$

ℓ_m = 48.1 millihenries referred to excitation winding

Calculations at 200 cps (400-Volt Winding)

X = blocked rotor reactance = $2\pi(200)\ell_{BR}$ = 8.45 ohms

X_o = no load reactance = $\frac{X}{2} + 2\pi(200)\ell_m$ = 64.5 ohms

$r_1 = r_{1x}$ = 5.96 ohms

$$r_2 = \left(\frac{N_x}{N_L}\right)^2 r_{2_L} = \left(\frac{252}{96}\right)^2 0.319 = 2.20 \text{ ohms}$$

E = volts/phase = 50 volts

m = phases = 2

FE = core loss = 2.37 watts (calculated from the magnetic circuit for a flux corresponding to 50 volts at 200 cps)

$$i_m = \frac{E}{X_o} = 0.775 \text{ amperes}$$

$$k_p = \sqrt{\frac{X_o - X}{X_o}} = 0.93$$

$$r_m = \frac{FE}{mi_m^2} = 1.98 \text{ ohms}$$

$$F_1 = X - \frac{r_m}{X_o} r_1 = 8.27$$

$$F_2 = r_2 = 2.20$$

$$F_3 = r_2 \frac{r_1 + r_m}{X_o} = 0.271$$

$$F_4 = r_1 + \frac{r_m}{X_o} X = 6.22$$

$F_5 = i_m r_m = 1.53$

$F_6 = i_m r_2 = 1.71$

$F_7 = Ek_p = 46.5$

S_m = slip at maximum torque = $\sqrt{\frac{F_2^2 + F_3^2}{F_1^2 + F_4^2}} = 0.214$

Syn = synchronous speed = 206 x 60 = 12,360 rpm

E.M.T. = Electro-magnetic torque = internal mechanical torque developed by the motor

The slips in the Table below are mostly measured slip values at 206 cps.

				Max.			
(1)	Slip: S	0.0242	0.0728	0.214	0.325	0.450	0.636
(2)	1/S	41.3	13.73	4.67	3.075	2.22	1.572
(3)	1 - S	0.976	0.927	0.786	0.675	0.55	0.364
(4)	(2) x F_3	11.2	3.72	1.27	0.83	0.60	0.430
(5)	F_1	8.27	8.27	8.27	8.27	8.27	8.27
(6)	u = (4) - (5)	2.93	-4.55	-7.00	-7.44	-7.67	-7.84
(7)	F_4	6.22	6.22	6.22	6.22	6.22	6.22
(8)	(2) x F_2	90.9	30.2	10.3	6.76	4.89	3.46
(9)	W = (7) + (8)	97.1	36.4	16.5	12.98	11.11	9.68
(10)	$\sqrt{U^2 + W^2}$	97.1	36.7	17.9	14.95	13.52	12.48
(11)	F_5	1.53	1.53	1.53	1.53	1.53	1.53
(12)	(2) x F_6	70.6	23.5	8.00	5.26	3.80	2.69
(13)	(11) + (12)	72.1	25.0	9.53	6.79	5.33	4.22
(14)	$\sqrt{(13)^2 + E^2}$	87.7	55.9	50.9	50.5	50.3	50.1
(15)	I_1 = (14)/(10)	0.903	1.52	2.85	3.38	3.72	4.02
(16)	$I_2 = F_7/(10)$	0.479	1.268	2.60	3.11	3.44	3.70
(17)	$I_2^2 F_2 m$	1.01	7.06	29.8	42.6	52.1	60.25
(18)	(17) x (2) x (3)	40.7	89.9	109.2	88.4	63.6	34.5
(19)	(3) x Syn	12,080	11,450	9,710	8,340	6,800	4,500
(20)	E.M.T. = $\frac{1350 \times (18)}{(19)}$ (in-oz)	4.57	10.6	15.2	14.3	12.6	10.3

Calculations at 400 cps (400-Volt Winding)

r_1, r_2, m, and K_p are the same as in the calculations at 200 cps.

i_m, r_m, and the "F" constants are calculated from the same equations.

$$X = 2\pi(400)\ell_{BR} = 16.9 \text{ ohms}$$

$$X_o = \frac{X}{2} + 2\pi(400)\ell_m = 129 \text{ ohms}$$

$$E = 115 \text{ volts}$$

FE = 7.3 watts (calculated from the magnetic circuit for a flux corresponding to 115 volts at 400 cps)

$$i_m = \frac{115}{129} = 0.890 \text{ amperes}$$

$$r_m = \frac{7.3}{2 \times (.89)^2} = 4.61 \text{ ohms}$$

$$F_1 = 16.9 - \frac{4.61}{129}\, 5.96 = 16.7$$

$$F_2 = 2.20$$

$$F_3 = 2.20\, \frac{5.96 + 4.61}{16.9} = 0.180$$

$$F_4 = 5.96 + \frac{4.61}{129}\, 16.9 = 6.56$$

$$F_5 = 0.890 \times 4.61 = 4.10$$

$$F_6 = 0.890 \times 2.20 = 1.96$$

$$Ek_p = 115 \times 0.93 = 107$$

$$S_m = \sqrt{\frac{2.20^2 + 0.180^2}{16.9^2 + 6.56^2}} = 0.122$$

SYN = 400 x 60 = 24,000 rpm

The slips in the Table below all correspond to measured slips at 400 cps.

(1)	Slip: S	0.015	0.035	0.060	0.090
(2)	1/S	66.7	28.6	16.7	11.1
(3)	1 - S	0.985	0.965	0.94	0.91
(4)	(2) x F_3	12.0	5.15	3.0	2.0
(5)	F_1	16.7	16.7	16.7	16.7
(6)	U = (4) - (5)	-4.7	-11.5	-13.7	-14.7
(7)	F_4	6.56	6.56	6.56	6.56
(8)	(2) x F_2	147	62.9	36.7	24.4
(9)	W = (7) + (8)	154	69.5	43.2	31.0
(10)	$\sqrt{U^2 + W^2}$	154	70.5	45.3	34.3
(11)	F_5	4.1	4.1	4.1	4.1
(12)	(2) x F_6	131	56.1	32.7	21.8
(13)	(11) + (12)	135	60.2	36.8	25.9
(14)	$\sqrt{(13)^2 + E^2}$	177.5	130	121	118
(15)	I_1 = (14)/(10)	1.15	1.84	2.67	3.44
(16)	$I_2 = F_7/(10)$	0.697	1.522	2.37	3.13
(17)	$I_2^2 F_2 m$	2.14	10.2	24.7	43.1
(18)	(17) x (2) x (3)	141	282	388	435
(19)	(3) x SYN	23,650	23,200	22,600	21,850
(20)	E.M.T. = $\frac{1350 \times (18)}{(19)}$ (in-oz)	8.05	16.4	23.2	26.8

11. Data from Alternator Tests

Notes:
1. Run 1 was made at a nominal speed of 18,000 rpm.
2. Run 2 was made at a nominal speed of 24,000 rpm.
3. In run 3 the excitation capacitances were decreased in steps with turbine input air kept constant.
4. Runs 4 and 5 were made at a nominal speed of 30,000 rpm.

5. In run 6 the excitation capacitances were decreased in steps as in run 3.
6. Runs 7 and 8 were made at a nominal speed of 36,000 rpm.
7. Run 9 was made at a nominal speed of 42,000 rpm. The complete data was not obtained because the bearing lubricant started to burn off one of the turbine bearings and speed had to be reduced.
8. In runs 10 and 11 the load resistances were decreased in steps with turbine input air kept constant.
9. The circuit diagram for alternator tests is shown in Figure 16.
10. In runs 1 through 3 load power was measured with a polyphase wattmeter. Two wattmeters were used in runs 4 through 11.
11. Load and excitation voltages were sinusoidal in each run.

The data is shown on the following page.

	Stator Freq. (cps)	Speed Rev/Sec	Excitation Capacitance Phase 1 (μf)	Excitation Capacitance Phase 2 (μf)	Excitation Voltage Phase 1 (Volts)	Excitation Voltage Phase 2 (Volts)	Excitation Current Phase 1 (Amps)	Excitation Current Phase 2 (Amps)	Load Voltage Phase 1 (Volts)	Load Voltage Phase 2 (Volts)	Load Current Phase 1 (Amps)	Load Current Phase 2 (Amps)	Load Power (Watts)	
Run 1	296	301	5.8	5.8	160	161	1.96	1.98	57.5	58	1.73	1.67	194	
	295	301	6.1	6.1	167	168	2.17	2.22	60	60	2.05	1.96	240	
	297	305	6.1	6.1	155	156	2.05	2.12	53.5	54	2.84	2.86	308	
Run 2	397	400	3.7	3.7	222	239	2.10	2.26	80.5	88	1.67	1.65	192	
	396	400	4.0	3.7	223	243	2.32	2.36	80	90	2.25	2.24	260	
Run 3	395	403	3.8	3.8	196	197	1.90	1.93	68.5	69	2.98	3.04	420	
	408	417	3.6	3.6	203	201	1.90	1.94	70	71	3.06	3.12	440	
	422	431	3.4	3.4	203	204	1.85	1.88	70.5	71	3.10	3.14	448	
	444	453	3.1	3.1	216	218	1.80	1.84	71.5	72	3.12	3.18	460	
													Phase 1 (Watts)	Phase 2 (Watts)
Run 4	492	498	2.5	2.5	299	300	2.37	2.43	105.5	107	2.25	2.20	247	240
Run 5	482	492	2.7	2.7	258	260	2.17	2.23	88	89	3.71	3.70	342	340
Run 6	498	505	2.4	2.4	258	260	1.95	2.00	89.5	91	2.86	2.85	268	268
	518	526	2.2	2.2	260	261	1.87	1.93	90	91	2.88	2.86	270	266
	546	554	2.0	2.0	261	264	1.80	1.85	91	92	2.90	2.90	276	273
Run 7	592	599	1.7	1.7	332	333	2.20	2.20	114.5	115.5	2.90	2.85	353	345
Run 8	592	600	1.8	1.8	350	352	2.42	2.46	121	122	3.25	3.23	417	415
Run 9		700	1.3	1.3	405	408	2.33	2.34	136	137.5			425	425
Run 10	495	500	2.4	2.4	285	288	2.15	2.24	102	103	1.97	1.90	210	205
	492	497	2.4	2.4	274	277	2.05	2.12	97.5	99	2.08	2.00	210	205
	489	495	2.4	2.4	255	258	1.88	1.95	91	92	2.25	2.20	210	207
Run 11	486	493	2.4	2.4	239	240	1.78	1.83	85	86	2.42	2.37	210	207
	490	498	2.4	2.4	220	221	1.63	1.67	77	78	2.63	2.70	209	212
	498	507	2.4	2.4	202	204	1.54	1.57	70	71	2.85	2.90	209	211
	510	521	2.4	2.4	190	189	1.45	1.50	64	65	3.10	3.10	210	210
	536	551	2.4	2.4	174	176	1.37	1.42	59	58	3.40	3.40	205	204

BIBLIOGRAPHY

Alger, P. L. The Nature of Polyphase Induction Machines. New York: John Wiley and Sons, 1951.

Dwight, H. B. Electrical Coils and Conductors. New York: McGraw-Hill Book Company, 1945.

Kuhlmann, J. H. Design of Electrical Apparatus. Second Edition, New York: John Wiley and Sons, 1940.

Roters, H. C. Electromagnetic Devices. New York: John Wiley and Sons, 1941.

Siskind, C. S. Alternating-Current Armature Windings. New York: McGraw-Hill Book Company, 1951.

Timoshenko, S. Strength of Materials. Part II, New York: Van Nostrand Company, Inc., 1940.

Appleman, W. R. "The Cause and Elimination of Noise in Small Motors", Electrical Engineering, Vol. 56 (November 1937), p. 1359.

Basset, E. D. and Potter, F. M. "Capacitor Excitation of Induction Generators", Electrical Engineering, Vol. 54 (May 1935), p. 540.

Hobart, H. M. and Knowlton, E. "The Squirrel Cage Induction Generator", AIEE Trans., Vol. 31, Pt. II (1912), pp. 1721-47.

Lyon, W. V. "Heat Losses in the Conductors of Alternating-Current Machines", AIEE Trans., Vol. 40 (1921), p. 1361.

Mikina, S. J. "Effect of Skewing and Pole Spacing on Magnetic Noise in Electrical Machinery", ASME Trans., Vol. 56 (October 1934), p. 711.

Taylor, H. W. "Eddy Currents in Stator Windings", JIEE, England, Vol. 58 (1920), p. 279.

Trickey, P. H. "Induction Motor Resistance Ring Width", Electrical Engineering, Vol. 55 (February 1936), p. 144.

Veinott, C. G. "Performance Calculations of Induction Motors", AIEE Trans., Vol. 51 (September 1932), p. 743.

Wagner, C. F. "Self Excitation of Induction Motors", AIEE Trans., Vol. 58 (1939).

Bross, R. B. of the Instrumentation Laboratory, M.I.T. Notes on Polyphase Induction Motor Design, Revised June 30, 1952.

Dwight, H. B. Notes for use with Course 6.25, Design of Electrical Machinery.

Estes, O. T. and Hussong, W. J. "Study of Capacitor Excited Induction Generators", M.I.T. Thesis, Naval Architecture, 1951.

"U.S.S. Electrical Steel Sheets - Engineering Manual No. 3", Pittsburgh, Carnegie-Illinois Steel Corp., 1949.